Copyright
by
Chun Biu Li
2003

The Dissertation Committee for Chun Biu Li
certifies that this is the approved version of the following dissertation:

Resonance Overlap, Secular Effects and Non-integrability: An Approach from Ensemble Theory

Committee:

Ilya Prigogine, Supervisor

Tomio Petrosky, Supervisor

Dean J. Driebe

E.C. George Sudarshan

Linda E. Reichl

Rafael de la Llave

Resonance Overlap, Secular Effects and Non-integrability: An Approach from Ensemble Theory

by

Chun Biu Li, B.S., M.S.

DISSERTATION

Presented to the Faculty of the Graduate School of

The University of Texas at Austin

in Partial Fulfillment

of the Requirements

for the Degree of

DOCTOR OF PHILOSOPHY

THE UNIVERSITY OF TEXAS AT AUSTIN

August 2003

Dedicated to my parents.

Acknowledgments

I wish to thank the multitudes of people who helped me. First I would like to express my sincere gratitude to Dr. Tomio Petrosky and Dr. Dean Driebe for supervising my research and dissertation, teaching me many aspects of how to and how not to do physics. In the past four years, they always have patient on me even when things were not going well. Of course, Prof. Prigogine's overall vision, generous encouragement and steady support have been the most important component of my education here. I would also like to thank Prof. George Sudarshan, Prof. Linda Reichl, Prof. Rafael de la Llave and Prof. Philip Morrison for their stimulative discussions. Finally I thank my parents for their support and encouragement.

Resonance Overlap, Secular Effects and Non-integrability: An Approach from Ensemble Theory

Publication No. _____

Chun Biu Li, Ph.D.
The University of Texas at Austin, 2003

Supervisors: Ilya Prigogine
Tomio Petrosky

The time evolution of classical multi-resonance non-integrable Hamiltonian systems with few degrees of freedom (the small Poincaré system) is analyzed on the ensemble level. In such systems, one encounters the small denominator problem in the traditional approach of trajectory dynamics. By applying the time-dependent perturbation analysis to the Liouville equation we can determine the most secular effects for the time evolution of the expectation value of some physical observables.

For the case of the large Poincaré system studied in non-equilibrium statistical mechanics with infinite degrees of freedom it is well known that the spectrum of the Liouville operator is continuous so that under the integration over the wave vector the small denominator can be treated as a distribution. On the other hand, the spectrum of the Liouville operator is discrete in the small Poincaré system. Therefore, it is necessary in this case to perform an

ensemble average over the continuous action variables for the small denominator to be treated as a distribution. In contrast to the so called $\lambda^2 t$-limit (the Van Hove limit) in non-equilibrium statistical mechanics for the large Poincaré system, we find $\sqrt{\lambda}t$-limit in the small Poincaré system. This shows that the resonance effect in the small Poincaré system is much stronger than in the large Poincaré system. In this limit, the time symmetry is broken as in non-equilibrium statistical mechanics. These secular effects exist only on the level of ensemble but not on the level of trajectory.

We are able to distinguish contributions from individual resonances and from the interference between the resonances. Since the interference is responsible for the non-integrability, one can now treat quantitatively the non-integrable effects on the level of ensemble. Our treatment of the interference effect naturally leads to the Chirikov overlapping criterion for the onset of global chaos. Comparison of our theoretical prediction to numerical simulation is excellent in the asymptotic time scale $t \sim 1/\sqrt{\lambda}$.

Table of Contents

List of Figures

Chapter 1

Introduction

In this thesis, we will analyze the time evolution of classical non-linear multi-resonance Hamiltonian systems with few degrees of freedom by using time-dependent perturbation analysis on the level of ensemble. We will call these Hamiltonian systems "small Poincaré systems", which are non-integrable in the sense of Poincaré [16], to distinguish them from large Poincaré systems with infinitely many degrees of freedom which have been extensively investigated in non-equilibrium statistical physics [1, 2, 17].

In the 1950's, Van Hove, Prigogine and his colleagues [7, 8, 17] applied asymptotic perturbation analysis to large Poincaré systems. They showed that by collecting the most diverging terms of t (the most secular effect) arising from the resonance effects in the asymptotic limit (the so called $\lambda^2 t$-limit with $t \to \infty$, $\lambda \to 0$ and keeping $\lambda^2 t$ finite, where λ is the coupling constant), one can derive kinetic equations that break time-symmetry. This important discovery has revealed a deeper relation between the origin of irreversibility in the basic laws of physics and the non-integrability of dynamical systems due to the resonance singularities. This has then led to remarkable developments of modern kinetic theory in non-equilibrium statistical physics, such as correla-

tion dynamics [17], subdynamics and non-unitary transformations [10–14, 18], complex spectral representation of the Hamiltonian and also of the Liouville-von Neumann operator outside the Hilbert space [3, 10, 12–15, 23, 24]. In this dissertation, we will develop the corresponding asymptotic perturbation analysis for small Poincaré systems.

It is well known that non-integrability leads to the failure of perturbation analysis on the level of trajectory due to the resonance singularity involved in each term of the perturbation series, i.e. the small denominator problem [9]. A way out of this difficulty, as will be shown, is to consider an ensemble average of an observable so that the small denominator can be treated as a distribution (generalized function) under the integration over the phase space variables.

The need to consider the small denominator under the integration over the phase space variables was recognized some years ago by Prigogine, Grecos and George [19]. By simply applying the kinetic theory developed for the large Poincaré systems in non-equilibrium statistical mechanics. One could expect that the same kinetic description might exist in the small Poincaré systems. However, this idea, while going into the right direction, is not enough to solve the small denominator problem in the small Poincaré systems. We find some differences in dealing with the small denominator problem in the small Poincaré systems from the large Poincaré systems.

In the case of large Poincaré systems, one may perform the integration over the continuous spectrum in each small denominator (propagator) which

is understood as an individual distribution in the continuous wave vectors. Hence a product of two propagators with two independent continuous wave vectors gives us a product of two ordinary functions after the integrations over the wave vectors.

On the other hand, in the case of small Poincaré systems, we have no integrations over the continuous spectrum of the Liouville operator. The small denominator is now understood as a distribution in the phase space variables (instead of the wave vectors) under the ensemble average over the phase space. As a result, a product of two propagators should be treated as a *single distribution* of the phase space variables, but not be treated as a product of two distributions depending on a single set of phase space variables. We will show in the text that the product of two propagators may lead to extra singularities of the resonances, which does not appear if we perform the integration over the continuous spectrum in each propagator as in the case of large Poincaré systems. These new singularities then lead to stronger secular effects in the small Poincaré systems than in the large Poincaré systems.

The above treatment of the small denominator is possible only on the level of ensemble but not on the level of trajectory. In other words, we are extracting some information of the dynamics which appears only on the ensemble level. One of the unique properties of the ensemble approach is the broken time symmetry.

The main contribution of this thesis are: (1) We find that the secular effect from each single resonance term is given by an asymptotic series with

time dependence $\lambda^{3/2}(\sqrt{\lambda}t)^{4m-3}$ for $m \geq 1$ in compared with the $(\lambda^2 t)^m$ contribution for the large Poincaré system. (2) We consider the contributions from the interference between the resonances and find the secular effects with oscillation corresponding to the higher harmonics of the system.

Since a single resonance system is integrable, one can expect that non-integrability of the multi-resonance system comes from the interference between the resonances. Therefore, it is convenient for us to consider the two contributions separately in order to contrast their properties.

In the consideration of the single resonance part, thanks to the integration over the phase space variables, we deduce a secular time dependence of $\lambda^{3/2}(\sqrt{\lambda}t)^{4m-3}$ from the resonance effect by considering the evolution of the expectation value of some observables.

A similar situation is also encountered for the interference part. Since the interference part contains propagators of different resonance points, we will see that the interference of propagators from different resonances generates extra poles which corresponds to the higher harmonics of the system. This leads to a secular effect with oscillation in the interference case.

It is also interesting to compare the secular effect of the single resonance part with that of the interference part. For a system with well-separated resonance points, one may expect that the interference part gives a small correction to the single resonance effects. However, the consistent estimation of the interference part is important no matter how small it is since this is the

first non-trivial correction that comes from the non-integrability of the system.

On the other hand, in the strongly-coupled case when the resonance points are close to each other the interference effect starts to dominate. One can no longer treat the interference part as a correction to the single resonance secular effects. We will see that our treatment of the interference effect naturally leads to the Chirikov overlapping criterion for the onset of global chaos [5]. It is interesting that we obtain this criterion by analyzing the secular effects on the level of ensemble theory.

The structure of this thesis is as follows:

In order to present our analysis, we will introduce a specific system as a working example with two resonance interactions in Chapter 2. Despite its simplicity, we will show that this system is non-integrable in the sense of Poincaré because it possesses infinitely many higher order resonances implicitly. For convenience, a discussion of the Poincaré's theorem on the non-existence of uniform invariants will be given in Appendix A. The appearance of higher order resonances will be shown both analytically from a suitable canonical transformation on the phase space variables and numerically from the Poincaré surface of section. Next, we will discuss the small denominator problem in the perturbation analysis on the level of trajectory which prevents the existence of uniform invariants due to the resonances [17, 25]. We will then discuss the way to solve this problem on the ensemble level.

In Chapter 3, we will discuss the Liouvillian formalism for ensemble the-

ory. The method we use to study the Liouville equation is the time-dependent perturbation analysis. We will carry out the perturbation analysis using the resolvent method [17].

We will start our perturbation analysis in Chapter 4. First we will separate the contribution into two parts, the single resonance part and the resonance interference part. The single resonance part corresponds to the contribution from each resonance without the presence of the other. The asymptotic expansion for the single resonance part will be derived in this Chapter. We will also show the agreement of our theoretical calculation with the numerical simulation.

In Chapter 5. we will consider the contribution from the interference between the resonances. The secular effects with oscillation will be derived and related to the higher harmonics of system. We will then comment on the connection of our result with the Chirikov overlapping criterion by comparing the secular effect of the single resonance case with the interference case. Our theoretical result for the interference part is again compared to the numerical simulation.

In Chapter 6, We will show that the most secular effect we derived breaks time symmetry. Finally, we will summarize our study and discuss the direction of future work in Chapter 7.

Chapter 2

The System

2.1 The Hamiltonian

Without loss of generality, we will consider a non-linear Hamiltonian system with two degrees of freedom, whose Hamiltonian has two resonance terms given by

$$H(J_1, J_2, \theta_1, \theta_2) = H_0(J_1, J_2) + \lambda V_1(\theta_1) + \lambda V_2(\theta_1, \theta_2) \tag{2.1}$$

with

$$\begin{aligned} H_0 &= J_1^2/2 + \omega_2 J_2 \\ V_1(\theta_1) &= \cos\theta_1 \\ V_2(\theta_1, \theta_2) &= \cos(\theta_1 - \theta_2) \end{aligned} \tag{2.2}$$

where λ is the perturbation parameter and $\omega_2 > 0$. We consider the case of weak coupling $\lambda \ll 1$. The domain of the variables are given by $-\infty < J_1 < \infty$, $0 < J_2$ and $0 \leq \theta_i < 2\pi$ for $i = 1,\ 2$.

This Hamiltonian system, describing the motion of two coupled oscillators, is the simplest non-integrable model one can construct. Despite its simplicity, this Hamiltonian displays the typical features of the on-set of chaos. In fact, the Hamiltonian system in (2.2) has been the subject of consideration

by many authors in the past such as Chirikov [5], Escande [6], Chandre and Jauslin [4] and has proven to be a good platform to study the transition to chaos in Hamiltonian systems[1]. However, these considerations were all based on the trajectory point of view in which information of the system is extracted from the phase space structure. In this thesis, we shall analyze the dynamics on the level of ensemble based on the Liouville equation.

We will first discuss the qualitative properties of our system by looking at the Poincaré surface of section in the next section. It is found, both from the phase space structure and a suitable canonical transformation discussed in Section 2.3, that our system contains infinitely many resonances which implies non-integrability according to the Poincaré's theorem discussed in Appendix A. The resonance effect also leads to the small denominator problem (see Section 2.3) in the canonical perturbation analysis and prevents us from constructing the invariant of motion which agrees with the Poincaré's theorem. In the rest of the chapter, we will discuss the resonance effect that motivate us in considering the ensemble theory for non-integrable system.

We emphasize here that even though our discussion in this thesis only consider the particular Hamiltonian in (2.2), it can be seen that our constructions can be easily applied to more general Hamiltonian systems with more

[1]In fact, these authors considered the one-and-a-half dimensional time-dependent non-integrable Hamiltonian of the form $H = J_1^2/2 + \lambda\cos\theta_1 + \lambda\cos(\theta_1 - \omega_2 t)$. This Hamiltonian describing the motion of a simple pendulum driven by a periodic external force can be transformed to our two dimensional model (2.2) by introducing a new pair of action-angle variables (J_2, θ_2) such that $\theta_2 = \omega_2 t$.

than two resonance interactions and systems with more than two degrees of freedom.

2.2 The Qualitative Picture of the System

The generic character of motion of our system can be understood by looking at the Poincaré surface of section. We first write down the equation of motion for our system

$$\begin{aligned} \frac{dJ_1}{dt} &= \lambda \sin\theta_1 + \lambda \sin(\theta_1 - \theta_2) \\ \frac{dJ_2}{dt} &= -\lambda \sin(\theta_1 - \theta_2) \\ \frac{d\theta_1}{dt} &= J_1 \\ \frac{d\theta_2}{dt} &= \omega_2 \end{aligned} \tag{2.3}$$

The trajectories of our system lie on the three-dimensional surface $H =$ constant. Due to the linearity of the Hamiltonian in the action variable J_2, the angle variable θ_2 is periodic with period $2\pi/\omega_2$ as can been seen from (2.3). Therefore we can construct the stroboscopic plot of the phase space with coordinate $\{J_1, \theta_1\}$ which corresponds to the orbits of the system at time $t = 2n\pi/\omega_2$, $n = 1, 2, \cdots$ so that $\theta_2 = 2\pi$. Such plot is a special type of Poincaré surface of section and has dimension of two in our case.

Figure 2.1a) shows the numerically integrated orbits for our system with $\lambda = 0.01$ and $\omega_2 = 0.8$. The two primary separatrices are well separated from each other and correspond to the resonance points at $J_1 = 0$ and $J_1 = \omega_2 = 0.8$ respectively. Besides the primary resonance, higher order res-

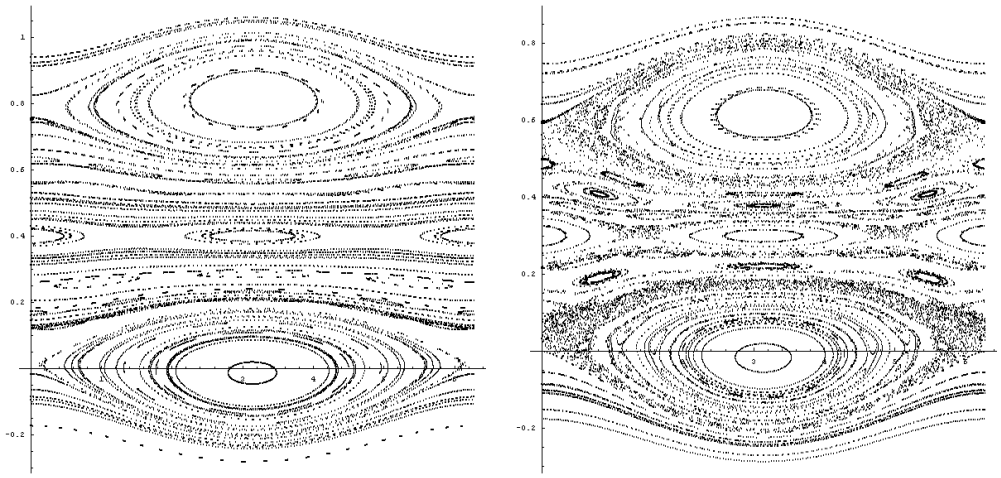

(a) $\omega_2 = 0.8$ (b) $\omega_2 = 0.6$

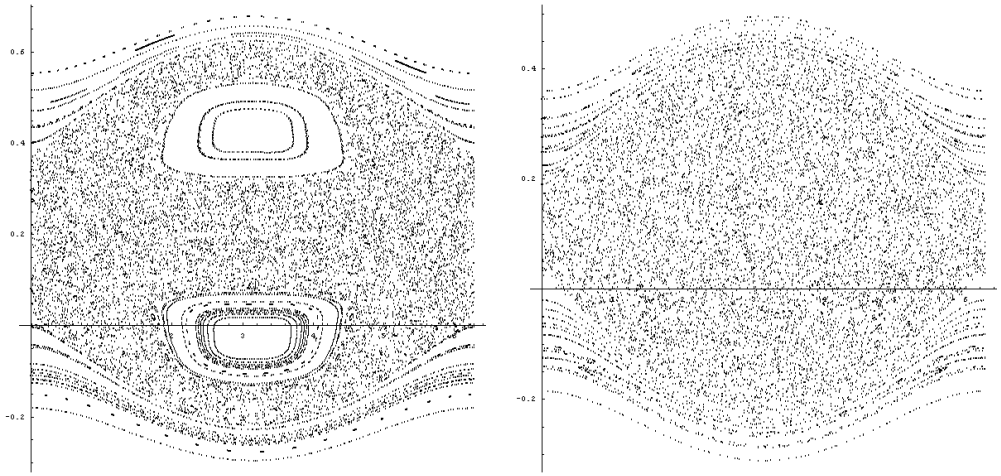

(c) $\omega_2 = 0.4$ (d) $\omega_2 = 0.2$

Figure 2.1: The Poincaré surface of sections of our system with $\lambda = 0.01$, the horizontal and vertical axis is θ_1 and J_1 respectively.

onances also appear in the diagram due to the interference between the two resonance terms in the Hamiltonian (2.2). Since the separation between the two primary resonances are still big compared to the widths of the separatrices in Figure 2.1a), an orbit started near the separatrices seems to remain in the neighborhood of that separatrix, therefore no chaos is visible yet.

If we decrease the distance ω_2 between the primary resonances as in Figure 2.1b), the resonances start to overlap and seriously interfere with each other so that trajectories start close to one separatrix can no longer stay in the neighborhood of the same separatrix, As a result, chaotic regions appear between the separatrices and leads to a phase space with a mixture of regular and chaotic motions. However, different chaotic regions are still isolated from each other by the regular motion (the so called KAM tori [9]) between them.

As we further reduce the distance between the resonances as in Figure 2.1c), the interference between the resonance becomes so strong that most of the regular orbits are destroyed. This results in the merge of different chaotic regions in the phase space. Further decreasing of ω_2 as in Figure 2.1d) eventually leads to fully chaotic motion.

2.3 Non-integrability: Appearance of Infinitely Many Resonances

Although the Hamiltonian system defined in (2.2) contains only two resonance terms, we see from the stroboscopic plot in the last section that many higher order resonances exist between the primary resonances. In fact,

it can be shown that there are infinitely many resonances densely distributed in any region of the action variable space due to the interference between the two resonance terms. To see this explicitly, we rewrite the Hamiltonian (2.2) in the form

$$H(J_1, J_2, \theta_1, \theta_2) = H_p(J_1, \theta_1) + \omega_2 J_2 + \lambda \cos(\theta_2 - \theta_2) \tag{2.4}$$

where $H_p(J_1, \theta_1) = J_1^2/2 + \lambda \cos\theta_1$ is the Hamiltonian of the one dimensional simple pendulum. Now, with $\{J_2, \theta_2\}$ unchanged, we canonically transform the set of the coordinates $\{J_1, \theta_1\}$ of the simple pendulum Hamiltonian to a new set of action-angle variables $\{J_1', \theta_1'\}$ such that the transformed Hamiltonian $H_p'(J_1')$ depends only on the new action variable J_1'. The full Hamiltonian (2.4) can then be expressed in terms of the new set of phase space variables $\{J_1', J_2, \theta_1', \theta_2\}$ as

$$H'(J_1', J_2, \theta_1', \theta_2) = H_p'(J_1') + \omega_2 J_2 + \lambda \cos(\theta_1(J_1', \theta_1') - \theta_2) \tag{2.5}$$

where we have expressed the old angle variable θ_1 in terms of the new set of canonical variables $\{J_1', \theta_1'\}$. It is seen that the Hamiltonian (2.5) contains infinitely many resonance terms if the interaction $\cos(\theta_1(J_1', \theta_1') - \theta_2)$ is Fourier expanded in the angle variables $\{\theta_1', \theta_2\}$

$$\begin{aligned} H'(J_1', J_2, \theta_1', \theta_2) &= H_p'(J_1') + \omega_2 J_2 + \lambda \cos(\theta_1(J_1', \theta_1') - \theta_2) \\ &= H_p'(J_1') + \omega_2 J_2 + \lambda \sum_{n_1, n_2} V_{n_1, n_2}(J_1', J_2) e^{i(n_1\theta_1' + n_2\theta_2)} \end{aligned} \tag{2.6}$$

with

$$V_{n_1, n_2}(J_1', J_2) = \frac{1}{(2\pi)^2} \int_0^{2\pi} d\theta_1' \int_0^{2\pi} d\theta_2 e^{-i(n_1\theta_1' + n_2\theta_2)} \cos(\theta_1(J_1', \theta_1') - \theta_2) \tag{2.7}$$

Therefore, according to the Poincaré's theorem (see Appendix A), we conclude that our system (2.2) is non-integrable such that no uniform invariant exists. This means that other than the Hamiltonian, there is no invariant of motion which is single-valued and regular in $J_1, J_2, \theta_1, \theta_2$ and λ.

2.4 Canonical Transformation: Small Denominator Problem

The absence of a second uniform invariant in our system can also be understood in terms of the small denominator problem appearing in the canonical perturbation expansion of trajectory dynamics. We sketch the idea as follow: Let us consider again our system in the form (2.6)

$$H(J_1, J_2, \theta_1, \theta_2) = H_0(J_1, J_2) + \lambda \sum_{n_1, n_2} V_{n_1, n_2}(J_1, J_2) e^{i(n_1\theta_1 + n_2\theta_2)} \tag{2.8}$$

where $H_0(J_1, J_2) = H_p(J_1) + \omega_2 J_2$. Here and henceforth, we will drop the "prime" in (2.6) and (2.7) for convenience. We then look for a canonical transformation $\{J_1, J_2, \theta_1, \theta_2\} \to \{J_1', J_2', \theta_1', \theta_2'\}$ such that the transformed Hamiltonian $H'(J_1', J_2')$ is cyclic, i.e. it depends only on the transformed action variables $\{J_1', J_2'\}$. Such a transformation can be found by expanding the generating function of the canonical transformation in powers of the small parameter λ and then solving the Hamilton-Jacobi equation successively to each power [9].

Instead of going into the detail of its derivation, we demonstrate our idea by just writing down the perturbation series for the transformation of J_1

up to first order in λ

$$J_1' = J_1 + \lambda \sum_{n_1,n_2} \frac{n_1 V_{n_1,n_2}(J_1, J_2)}{n_1\Omega_1(J_1) + n_2\Omega_2(J_2)} e^{i(n_1\theta_1 + n_2\theta_2)} + \cdots \tag{2.9}$$

where $\Omega_1(J_1) = \partial H_0(J_1, J_2)/\partial J_1$ and $\Omega_2(J_2) = \partial H_0(J_1, J_2)/\partial J_2$ are the unperturbed frequencies. We are now faced with the problem of small denominators, since for any J_1 and J_2, a pair of integers n_1 and n_2 can be found such that $n_1\Omega_1(J_1)+n_2\Omega_2(J_2)$ is arbitrarily close to zero. This clearly prevents the series from converging and spoils the existence of uniform invariants as concluded by the Poincaré's theorem. Hence, on the level of trajectory dynamics, the perturbation expansion (2.9) loses its meaning.

However, let us suppose the expression (2.9) appears under the integration over the action variables with a suitable distribution function. Then, thanks to the non-linearity of H_0, the denominator in (2.9) has a legitimate meaning as a Cauchy integral by adding a complex number $-z$ to the denominator as $(n_1\Omega_1(J_1) + n_2\Omega_2(J_2) - z)^{-1}$ [1]. The expression (2.9) can then be understood as the value of the Cauchy integral at $z = 0$. Since the Cauchy integral is generally a multi-valued function on the real axis of z, the value of (2.9) depends on the way to perform the analytic continuation of z from the upper-half plane, or from the lower-half plane. An important aspect of this view of the denominator is that one can consistently deal with the resonance singularity at $n_1\Omega_1(J_1) + n_2\Omega_2(J_2) = 0$ under the integration over the continuous action variables $\vec{J}$. The denominator is no more a simple function but a distribution, i.e. a generalized function. However, the effect of the resonance

appears as a distribution can only be found on the level of ensemble, but not on the level of trajectories. On the other hand, the possibility of the two directions of the analytic continuation mentioned above leads to an important consequence, the broken time symmetry on the level of ensemble.

In the following chapters we will develop the ensemble approach of the non-linear dynamics with a few degrees of freedom based on the Liouville equation.

Chapter 3

Liouvillian Formalism

3.1 The Liouville Equation

The system we considered is a classical Hamiltonian system with two degrees of freedom and described by the action-angle variables. The Hamiltonian (2.2) of the system is decomposed into the integrable part $H_0(\vec{J})$ and the perturbation part $\lambda V(\vec{J},\vec{\theta})$, where we have used the vector notation $\vec{J} = \{J_1, J_2\}$ and $\vec{\theta} = \{\theta_1, \theta_2\}$ for the action and angle variables.

Instead of following the trajectory of the system in the phase space, we consider the ensemble theory of the system which focuses on the time evolution of the probability density $\rho(\vec{J},\vec{\theta},t)$. The probability density satisfies the Liouville equation [17],

$$i\frac{\partial\rho(\vec{J},\vec{\theta},t)}{\partial t} = L\rho(\vec{J},\vec{\theta},t) \tag{3.1}$$

The Liouville operator L is defined by the Poisson bracket $L = i\{H, \}$. Here the factor i is introduced to make L Hermitian in the Hilbert space where the inner product of the phase space functions $f(\vec{J},\vec{\theta})$ and $g(\vec{J},\vec{\theta})$ is defined by

$$(f,g) \equiv \int d\vec{J}d\vec{\theta}f^*(\vec{J},\vec{\theta})g(\vec{J},\vec{\theta}) \tag{3.2}$$

where $*$ means the complex conjugate. With a Hamiltonian that is decomposed as $H = H_0 + \lambda V$, L is decomposed into

$$L = L_0 + \lambda \delta L \tag{3.3}$$

where

$$L_0 = -i\vec{\Omega} \cdot \frac{\partial}{\partial \vec{\theta}} \tag{3.4}$$

$$\delta L = i\left[\frac{\partial V}{\partial \vec{\theta}} \cdot \frac{\partial}{\partial \vec{J}} - \frac{\partial V}{\partial \vec{J}} \cdot \frac{\partial}{\partial \vec{\theta}}\right] \tag{3.5}$$

with $\vec{\Omega} = \{\Omega_1, \Omega_2\} = \{\partial H_0/\partial J_1, \partial H_0/\partial J_2\}$, $\partial/\partial\vec{\theta} = \{\partial/\partial\theta_1, \partial/\partial\theta_2\}$ and so on. Also we have used the notation $\vec{\alpha} \cdot \vec{\beta} = \alpha_1\beta_1 + \alpha_2\beta_2$.

Since the unperturbed motion is integrable, the eigenspectrum of L_0 can be found easily as

$$L_0\Phi_{\vec{n}}(\vec{\theta}) = (\vec{n} \cdot \vec{\Omega})\Phi_{\vec{n}}(\vec{\theta}) \tag{3.6}$$

with eigenfunction

$$\Phi_{\vec{n}}(\vec{\theta}) = \frac{1}{2\pi} e^{i\vec{n}\cdot\vec{\theta}} = \langle\vec{\theta}|\vec{n}\rangle \tag{3.7}$$

where $|\vec{n}\rangle = |n_1, n_2\rangle$ denotes the eigenket of L_0 with any integers, n_1 and n_2. The completeness and orthonormality relation of the eigenvectors are

$$\sum_{\vec{n}} |\vec{n}\rangle\langle\vec{n}| = 1 \tag{3.8}$$

$$\langle\vec{n}|\vec{n}'\rangle = \delta_{\vec{n},\vec{n}'} \tag{3.9}$$

where $\Sigma_{\vec{n}} = \Sigma_{n_1}\Sigma_{n_2}$ and $\delta_{\vec{n},\vec{n}'} = \delta_{n_1,n_1'}\delta_{n_2,n_2'}$.

In the following discussions, the matrix elements of an operator L will be used frequently and is defined as

$$\langle \vec{n}|L|\vec{n}'\rangle = \int_0^{2\pi} d\theta_1 \int_0^{2\pi} d\theta_2 \Phi^*_{\vec{n}}(\vec{\theta}) L \Phi_{\vec{n}'}(\vec{\theta}) \tag{3.10}$$

so we have

$$\langle \vec{n}|L_0|\vec{n}'\rangle = (\vec{n}\cdot\vec{\Omega})\delta_{\vec{n},\vec{n}'} \tag{3.11}$$

and

$$\langle \vec{n}|\delta L|\vec{n}'\rangle = -V_{\vec{n}-\vec{n}'}(\vec{J})\vec{n}\cdot\frac{\partial}{\partial \vec{J}} + (\vec{n}'\cdot\frac{\partial}{\partial \vec{J}})V_{\vec{n}-\vec{n}'}(\vec{J}) \tag{3.12}$$

where $V_{\vec{n}}(J)$ is the Fourier component of the interaction in the Hamiltonian (2.2).

3.2 The Resolvent Method

As mentioned in Introduction, the Liouville equation will be studied by the time-dependent perturbation theory. In order to do that, we employ the resolvent method in which the Liouville equation (3.1) is solved formally in terms of the resolvent operator [17] by Laplace transformation as

$$\rho(\vec{J},\vec{\theta},t) = e^{-iLt}\rho(\vec{J},\vec{\theta},0) = \frac{-1}{2\pi i}\int_C dz e^{-izt} R(z)\rho(\vec{J},\vec{\theta},0) \tag{3.13}$$

where e^{-iLt} is the time evolution operator and $R(z) = 1/(L-z)$ is the resolvent operator. The contour C lies above the real axis of z and goes from ∞ to $-\infty$ for $t > 0$. As the Liouville operator L is Hermitian and has only real eigenvalues, the only singularities of the resolvent $R(z)$ are on the real-z axis. Moreover, due to the exponential factor $\exp(-izt)$ with $t > 0$ in (3.13), we

may close the contour of the integration by a large semicircle in the lower half plane. As a result, the asymptotic behavior of (3.13) is given by the residue of the poles of the resolvent operator on the real-z axis.

Since the distribution function $\rho(\vec{J},\vec{\theta},t)$ is a periodic function of the angle variable, we then expand it as a Fourier series,

$$\rho(\vec{J},\vec{\theta},t)=\left(\frac{1}{2\pi}\right)^2\sum_{\vec{n}}\rho_{\vec{n}}(\vec{J},t)e^{i\vec{n}\cdot\vec{\theta}} \tag{3.14}$$

After substituting (3.14) into (3.13), we then have the formal solution for the evolution of the Fourier mode $\rho_{\vec{n}}(\vec{J},t)$ as

$$\rho_{\vec{n}}(\vec{J},t)=\frac{-1}{2\pi i}\int_C dz e^{-izt}\sum_{\vec{n}'}\langle\vec{n}|\frac{1}{L-z}|\vec{n}'\rangle\rho_{\vec{n}'}(\vec{J},0) \tag{3.15}$$

In order to simplify our calculation, we will consider the situation in which the initial distribution function $\rho(\vec{J},\vec{\theta},t=0)$ is independent of the angle variables, i.e.

$$\rho_{\vec{n}}(\vec{J},t=0)=0 \qquad \text{if} \qquad \vec{n}\neq\vec{0} \tag{3.16}$$

which means that the initial distribution function is homogeneous in the angle variable. Note that this condition does not persist for $t>0$ due to the interactions. We will also assume that the initial distribution function is analytic in any finite domain of $\vec{J}$.

As mentioned in Introduction and last chapter, we are interested in the time evolution of the ensemble average of observables. Again, for the purpose of simplicity, let us consider observables $A(\vec{J})$ which depend only on the action

variables $\vec{J}$ and are analytic in any finite domain of $\vec{J}$. We then have

$$\begin{aligned}\langle A(\vec{J})\rangle_t &= \int d^2Jd^2\theta A(\vec{J})\rho(\vec{J},\vec{\theta},t) \\ &= \left(\frac{1}{2\pi}\right)^2 \int d\vec{J}d\vec{\theta}A(\vec{J})\sum_{\vec{n}}\rho_{\vec{n}}(\vec{J},t)e^{i\vec{n}\cdot\vec{\theta}} \\ &= \int d^2JA(\vec{J})\rho_{\vec{0}}(\vec{J},t)\end{aligned} \tag{3.17}$$

where $d^2J = dJ_1dJ_2$ and $d^2\theta = d\theta_1 d\theta_2$. We see that $\langle A(\vec{J})\rangle_t$ only depends on the evolution of the zeroth Fourier mode of the distribution function $\rho_{\vec{0}}(\vec{J},t)$.

With the above simplifications and using (3.15), the evolution of the $\langle A(\vec{J})\rangle_t$ is then given by (3.17)

$$\langle A(\vec{J})\rangle_t = \frac{-1}{2\pi i}\int d^2JA(\vec{J})\int_C dze^{-izt}\langle\vec{0}|\frac{1}{L-z}|\vec{0}\rangle\rho_{\vec{0}}(\vec{J},0) \tag{3.18}$$

Now perturbation analysis can be carried out by using the operator identity [17]

$$\frac{1}{L-z} = \frac{1}{L_0+\lambda\,\delta L - z} = \sum_{k=0}^{\infty}(-\lambda)^k\frac{1}{L_0-z}\left(\delta L\frac{1}{L_0-z}\right)^k \tag{3.19}$$

After substituting (3.19) into (3.18) and using the completeness relation (3.8), the expectation value $\langle A(\vec{J})\rangle_t$ becomes

$$\begin{aligned}\langle A(\vec{J})\rangle_t = \frac{-1}{2\pi i}\int d^2JA(\vec{J})\int_C dze^{-izt}\sum_{k=0}^{\infty}(-\lambda)^k\sum_{\vec{n}^{(1)},\vec{n}^{(2)},\cdots,\vec{n}^{(k-1)}}\frac{1}{z^2} \\ \times\langle\vec{0}|\delta L|\vec{n}^{(k-1)}\rangle\frac{1}{\vec{n}^{(k-1)}\cdot\vec{\Omega}-z}\langle\vec{n}^{(k-1)}|\delta L|\vec{n}^{(k-2)}\rangle\frac{1}{\vec{n}^{(k-2)}\cdot\vec{\Omega}-z}\cdots \\ \times\langle\vec{n}^{(2)}|\delta L|\vec{n}^{(1)}\rangle\frac{1}{\vec{n}^{(1)}\cdot\vec{\Omega}-z}\langle\vec{n}^{(1)}|\delta L|\vec{0}\rangle\rho_{\vec{0}}(\vec{J},0)\end{aligned} \tag{3.20}$$

where $\Sigma_{\vec{n}^{(1)},\vec{n}^{(2)},\cdots,\vec{n}^{(k-1)}} = \Sigma_{\vec{n}^{(1)}}\Sigma_{\vec{n}^{(2)}}\cdots\Sigma_{\vec{n}^{(k-1)}}$, and we have used the fact that $|\vec{n}^{(i)}\rangle$ is the eigenstate of the unperturbed Liouville operator L_0 with eigenvalue $\vec{n}^{(i)}\cdot\vec{\Omega}$. It can be seen from (3.20) that the time evolution of the expectation value $\langle A(\vec{J})\rangle_t$ is determined by summing the contributions from all the allowable transitions that bring the initial state $|\vec{0}\rangle$ to the final state $|\vec{0}\rangle$. The resonance effect enters the calculation from the propagator $(\vec{n}^{(i)}\cdot\vec{\Omega}-z)^{-1}$, $i=1,2,\cdots,k-1$ for each intermediate state. In particular, we will see in the next chapter that by evaluating the residues of the poles of these propagators gives rise to the secular effects for the time evolution which breaks time symmetry.

Chapter 4

Perturbation Expansion and Effect of Resonances

In this chapter, we will start with (3.20) and perform the perturbation analysis to the expectation value of the observable $\langle A(\vec{J})\rangle_t$. In order to demonstrate our procedure more systematically, we will divide the terms in the series (3.20) into two parts, namely the part which corresponds to the contributions from each individual resonance term, and the part which corresponds to the contribution from the interference between the two resonances. Since the single resonance systems are integrable, one can expect that non-integrability of multi-resonance systems comes from the interference between the resonances. A detailed discussion of these separations will be given in Section 4.1. We will first perform the perturbation analysis to the single resonance part of the series in this chapter, and the interference part will be considered in the next chapter.

In Section 4.2.1 , the perturbation analysis will be carried out in the zeroth and first order. The second order calculation will be presented in Section 4.2.2 where we develop the mathematical tool in evaluating the most secular terms in the series (3.20). This method is found to be useful even in the inter-

ference case discussed in the next chapter. Up to the second order calculation, the secular effect coming from the resonance singularity is essentially the same as the well-known secular effect of $\lambda^2 t$-approximation of the large Poincaré system, which has been studied in detail in non-equilibrium statistical mechanics [17].

An important deviation from the large Poincaré system starts from the fourth order calculation presented in Section 4.2.3. We will show that the most secular time dependence of the small Poincaré system is different from that of the large Poincaré system. In the last section of this chapter, the most secular series of the single resonance part, which we call $\sqrt{\lambda}t$-expansion, will be derived and compared with the well-known $\lambda^2 t$-expansion of the large Poincaré system. For comparison, a brief review of the derivation of the $\lambda^2 t$-expansion of the large Poincaré system is given in Appendix B. Also, the Prigogine and Henin's diagrammatic representation will be adopted in the fourth and higher order calculations for convenience.

Before we turn to the discussion of the classification of the single resonance and interference part, let us first write down the Liouville operator of our Hamiltonian system (2.2) in the form

$$\begin{aligned} L &= L_0 + \lambda\delta L_1 + \lambda\delta L_2 \\ L_0 &= -i\vec{\Omega}\cdot\frac{\partial}{\partial\vec{\theta}} \\ \delta L_1 &= -i\frac{\partial V_1}{\partial\vec{\theta}}\cdot\frac{\partial}{\partial\vec{J}} = i\sin\theta_1\partial_1 \\ \delta L_2 &= -i\frac{\partial V_2}{\partial\vec{\theta}}\cdot\frac{\partial}{\partial\vec{J}} = i\sin(\theta_1-\theta_2)(\partial_1-\partial_2) \end{aligned} \tag{4.1}$$

where we have divided the perturbed Liouville operator δL into two parts δL_1 and δL_2 corresponding to the two resonance interactions in the Hamiltonian. This separation allows us to look at different aspects of the system more easily as will be discussed shortly. In (4.1) and henceforth, the notation $\partial_{1,2} \equiv \partial/\partial J_{1,2}$ and $\partial_{12} \equiv \partial_1 - \partial_2$ will be used. By applying the expression (3.12) to our system, we obtain the non-zero matrix elements of δL_1 and δL_2 as

$$\langle n_1, n_2|\delta L_1|n_1+1, n_2\rangle = -\langle n_1, n_2|\delta L_1|n_1-1, n_2\rangle = \frac{1}{2}\partial_1 \tag{4.2}$$

and

$$\langle n_1, n_2|\delta L_2|n_1+1, n_2-1\rangle = -\langle n_1, n_2|\delta L_2|n_1-1, n_2+1\rangle = \frac{1}{2}\partial_{12} \tag{4.3}$$

with all other matrix elements of δL_1 and δL_2 vanish. These matrix elements will be used frequently in the following chapters.

4.1 Single Resonance and Interference between Resonances

Let us consider the time evolution of the expectation value (3.18) with the operator expansion (3.19). Now, if we use the decomposition $\delta L = \delta L_1 +$

δL_2, we obtain

$$\begin{aligned}
\langle A(\vec{J})\rangle_t &= \frac{-1}{2\pi i}\int d^2J A(\vec{J})\int_C dz e^{-izt} \\
&\quad\times\sum_{k=0}^{\infty}(-\lambda)^k\langle\vec{0}|\frac{1}{L_0-z}\left((\delta L_1+\delta L_2)\frac{1}{L_0-z}\right)^k|\vec{0}\rangle\rho_{\vec{0}}(\vec{J},0) \\
&= \frac{-1}{2\pi i}\int d^2J A(\vec{J})\int_C dz e^{-izt}\Bigg[\langle\vec{0}|\frac{1}{L_0-z}|\vec{0}\rangle \\
&\quad+\sum_{k=1}^{\infty}(-\lambda)^k\langle\vec{0}|\frac{1}{L_0-z}\left(\delta L_1\frac{1}{L_0-z}\right)^k|\vec{0}\rangle \\
&\quad+\sum_{k=1}^{\infty}(-\lambda)^k\langle\vec{0}|\frac{1}{L_0-z}\left(\delta L_1\frac{1}{L_0-z}\right)^k|\vec{0}\rangle \\
&\quad+\sum_{k=1}^{\infty}(\text{terms included both }\delta L_1\text{ and }\delta L_2)\Bigg]\rho_{\vec{0}}(\vec{J},0)
\end{aligned} \tag{4.4}$$

One can then easily see that the first summation of terms including δL_1 only describes the time evolution of $\langle A(\vec{J})\rangle_t$ under the Hamiltonian

$$H_1(\vec{J},\vec{\theta}) = H_0(\vec{J}) + \lambda V_1(\vec{\theta}) \tag{4.5}$$

which corresponds to a single resonance at $J_1 = 0$, and is therefore integrable. Similarly, the second summation of terms in (4.4) containing only the operator δL_2 corresponds to the integrable Hamiltonian

$$H_2(\vec{J},\vec{\theta}) = H_0(\vec{J}) + \lambda V_2(\vec{\theta}) \tag{4.6}$$

which describes the resonance at $J_1 = \omega_2$. Therefore the terms containing either δL_1 or δL_2 (but not both) in (4.4) are called the single resonance part of the system and will be considered in this chapter.

On the other hand, the terms containing both δL_1 and δL_2 in (4.4) describe the interference between the two resonances. All interesting features

of chaotic behavior in our system come from the interference between the resonances and will be treated in detail in the next chapter.

We are now ready to evaluate the evolution of the single resonance part of the expectation value (4.4) order by order in λ.

4.2 Contribution from Single Resonance

4.2.1 Zeroth and First Order Contributions

From (3.20), the zeroth order term is just the unperturbed motion,

$$\begin{aligned}\langle A(\vec{J})\rangle_t^{(0)} &= \frac{-1}{2\pi i}\int d^2J A(\vec{J})\int_C dz e^{-izt}\langle\vec{0}|\frac{1}{L_0-z}|\vec{0}\rangle\rho_{\vec{0}}(\vec{J},0)\\ &= \frac{1}{2\pi i}\int d^2J A(\vec{J})\int_C dz\frac{e^{-izt}}{z}\rho_{\vec{0}}(\vec{J},0)\\ &= \int d^2J A(\vec{J})\rho_{\vec{0}}(\vec{J},0)\\ &= \langle A(\vec{J})\rangle_{t=0}\end{aligned} \tag{4.7}$$

where the superscript (0) indicates the order of approximation.

On the other hand, from the explicit form of the non-zero matrix elements in (4.2) and (4.3), we see that transitions from $|\vec{0}\rangle$ to $|\vec{0}\rangle$ in a single step are forbidden, i.e. $\langle\vec{0}|\delta L|\vec{0}\rangle = 0$ and therefore according to (3.20), the first order term vanishes, i.e. $\langle A(\vec{J})\rangle_t^{(1)} = 0$. Moreover, it is not hard to see that all odd order terms vanish because there is no transition from $|\vec{0}\rangle$ to $|\vec{0}\rangle$ in odd number of steps, i.e. the transition $\langle\vec{0}|\delta L|\vec{n}^{(k-1)}\rangle$, $\langle\vec{n}^{(k-1)}|\delta L|\vec{n}^{(k-2)}\rangle$, $\cdots$, $\langle\vec{n}^{(2)}|\delta L|\vec{n}^{(1)}\rangle$, $\langle\vec{n}^{(1)}|\delta L|\vec{0}\rangle$ is forbidden for odd k in our system.

4.2.2 Second Order Contribution: Evaluation of Secular Effect

In second order, it is easy to see that the non-vanishing contributions come only from the single resonance part in (4.4) as

$$\begin{aligned}\langle A(\vec{J})\rangle_t^{(2)} = \frac{\lambda^2}{2\pi i}\int d^2J A(\vec{J})\int_C dz e^{-izt}\left(\frac{1}{2z}\right)^2 \sum_{n=\pm 1}\Bigg[\partial_1 \frac{1}{nJ_1 - z}\partial_1 \\ + \partial_{12}\frac{1}{n(J_1-\omega_2)-z}\partial_{12}\Bigg]\rho_{\vec{0}}(\vec{J},0)\end{aligned} \tag{4.8}$$

where the first term inside the square bracket comes from the transition in (4.2) and the second term comes from those in (4.3).

To extract the most secular terms from this expression, let us first follow the procedure similar to the derivation of the $\lambda^2 t$-approximation for the large Poincaré system (see Appendix B). It is well known that the most secular effect corresponds to the asymptotic limit $z \to i0^+$ [17], so by using the identity $\lim_{\epsilon\to 0^+}(1/(J-i\epsilon) - 1/(J+i\epsilon)) = 2\pi i\delta(J)$, (4.8) becomes

$$\begin{aligned}\langle A(\vec{J})\rangle_t^{(2)} &\sim \frac{\lambda^2\pi i}{2}\int d^2J A(\vec{J}) \operatorname*{Res}_{z=i0^+}\left[\frac{e^{-izt}}{z^2}\right](\partial_1\delta(J_1)\partial_1 \\ &\quad + \partial_{12}\delta(J_1-\omega_2)\partial_{12})\rho_{\vec{0}}(\vec{J},0) \\ &\sim \frac{-\lambda^2 t\pi}{2}\Bigg[\int dJ_2(\partial_1 A(\vec{J}))(\partial_1\rho_{\vec{0}}(\vec{J},0))\Big|_{J_1=0} \\ &\quad + \int dJ_2(\partial_{12}A(\vec{J}))(\partial_{12}\rho_{\vec{0}}(\vec{J},0))\Big|_{J_1=\omega_2}\Bigg]\end{aligned} \tag{4.9}$$

where $\sim$ means the most secular terms (i.e. terms containing the highest power in t), and any other contributions have been ignored. So we see that in the second order approximation, the most secular time dependence $\lambda^2 t$ is the same as the $\lambda^2 t$-expansion of the large Poincaré system.

However, we note that without the integration over the action variables, the second order term diverges at the resonance point $J_1 = 0$ and $J_1 = \omega_2$ due to the delta function (i.e. the small denominator problem). The consideration of the expectation value under the integration over the action variables solves this problem and gives us definite result by picking up the pole contributions from the resonance points.

As pointed out in Introduction, we will see that the above approach does not work in higher order due to the appearance of the product of the delta functions. Therefore we manipulate (4.8) by a different approach to extract the same most secular terms as in the last expression (4.9). After summing over n in (4.8), we have

$$\begin{aligned}\langle A(\vec{J})\rangle_t^{(2)} = \frac{\lambda^2}{2^2\pi i}\int d^2J \int_C dz \frac{e^{-izt}}{z} A(\vec{J})\Big[\partial_1 \frac{1}{J_1^2 - z^2}\partial_1 \\ + \partial_{12}\frac{1}{(J_1-\omega_2)^2 - z^2}\partial_{12}\Big]\rho_{\vec{0}}(\vec{J},0)\end{aligned} \tag{4.10}$$

Note that we can obtain the same result in (4.9) by first evaluating the residue of the factors $1/(J_1^2 - z^2)$ and $1/((J_1 - \omega^2)^2 - z^2)$ at the poles on the upper half complex-J_1 plane. Indeed, if we define the contribution from the residues

at the resonance points of (4.10) as

$$
\begin{aligned}
[\langle A(\vec{J})\rangle_t^{(2)}]_R \equiv \frac{\lambda^2}{2^2\pi i}(2\pi i)^2 \Bigg\{ & \operatorname*{Res}_{z=i0} \operatorname*{Res}_{J_1=z} \left[\int dJ_2 \frac{e^{-izt}}{z} A(\vec{J}) \partial_1 \frac{1}{J_1^2 - z^2} \partial_1 \rho_{\vec{0}}(\vec{J}, 0) \right] \\
& + \operatorname*{Res}_{z=i0} \operatorname*{Res}_{J_1=\omega_2+z} \left[\int dJ_2 \frac{e^{-izt}}{z} A(\vec{J}) \partial_{12} \frac{1}{(J_1 - \omega_2)^2 - z^2} \partial_{12} \rho_{\vec{0}}(\vec{J}, 0) \right] \Bigg\} \\
\sim \frac{-\lambda^2 t\pi}{2} \Bigg[& \int dJ_2 (\partial_1 A(\vec{J}))(\partial_1 \rho_{\vec{0}}(\vec{J}, 0)) \Big|_{J_1=0} \\
& + \int dJ_2 (\partial_{12} A(\vec{J}))(\partial_{12} \rho_{\vec{0}}(\vec{J}, 0)) \Big|_{J_1=\omega_2} \Bigg]
\end{aligned}
\tag{4.11}
$$

where the subscript R in $[\langle A(\vec{J})\rangle_t^{(2)}]_R$ denote that it comes from the residues. By comparing this result with (4.9), we have $\langle A(\vec{J})\rangle_t^{(2)} \sim [\langle A(\vec{J})\rangle_t^{(2)}]_R$ in (4.11). The advantage of this procedure is that one can avoid the appearance of the product of the delta function. In the following sections, we will apply this procedure to the higher order calculations.

4.2.3 Fourth Order Contribution: Use of Diagrammatic Representation

From (3.20), the fourth order term is

$$
\begin{aligned}
\langle A(\vec{J})\rangle_t^{(4)} = \frac{-\lambda^4}{2\pi i} \int d^2J A(\vec{J}) \int_C dz e^{-izt} & \sum_{\vec{n}^{(1)}, \vec{n}^{(2)}, \vec{n}^{(3)}} \frac{1}{z^2} \\
& \times \langle \vec{0} | \delta L | \vec{n}^{(3)} \rangle \frac{1}{\vec{n}^{(3)} \cdot \vec{\Omega} - z} \langle \vec{n}^{(3)} | \delta L | \vec{n}^{(2)} \rangle \frac{1}{\vec{n}^{(2)} \cdot \vec{\Omega} - z} \\
& \times \langle \vec{n}^{(2)} | \delta L | \vec{n}^{(1)} \rangle \frac{1}{\vec{n}^{(1)} \cdot \vec{\Omega} - z} \langle \vec{n}^{(1)} | \delta L | \vec{0} \rangle \rho_{\vec{0}}(\vec{J}, 0)
\end{aligned}
\tag{4.12}
$$

This expression is much more complex than that in the second order contribution. In order to organize the allowable transitions of the above expression

in a systematic way, we adopt the Prigogine and Henin's diagrammatic representation [20, 21] in the following discussion.

According to this representation, the transitions $\langle \vec{n}^{(i+1)} | \delta L | \vec{n}^{(i)} \rangle$ in (3.20) are represented by vertices attached by directed lines, and the propagators $(\vec{n}^{(i)} \cdot \vec{\Omega} - z)^{-1}$ are represented by directed lines with labels. We give the detailed description of the diagrammatic representation for the system we considered in Appendix C.

Using the diagrammatic representation, we list all allowable transitions of (4.12) in terms of their diagrams in Figure 4.1 . In Figure 4.1, the diagrams are grouped according to their topological difference. Since the transitions from the single resonance part of the dynamics come from each individual resonance, they are represented by the "single resonance diagrams" which involve only one type of vertices from a single resonance. These diagrams are given in Figure 4.1a)-b). The transitions represented by the "interference diagrams" in Figure 4.1c)-e) involve vertices from both resonances and correspond to the interference part of the dynamics. These interference diagrams and their secular time dependence will be discussed in next chapter.

Let us first consider the four diagrams listed in the first line of Figure 4.1a) which come from the single resonance at $J_1 = 0$. The corresponding

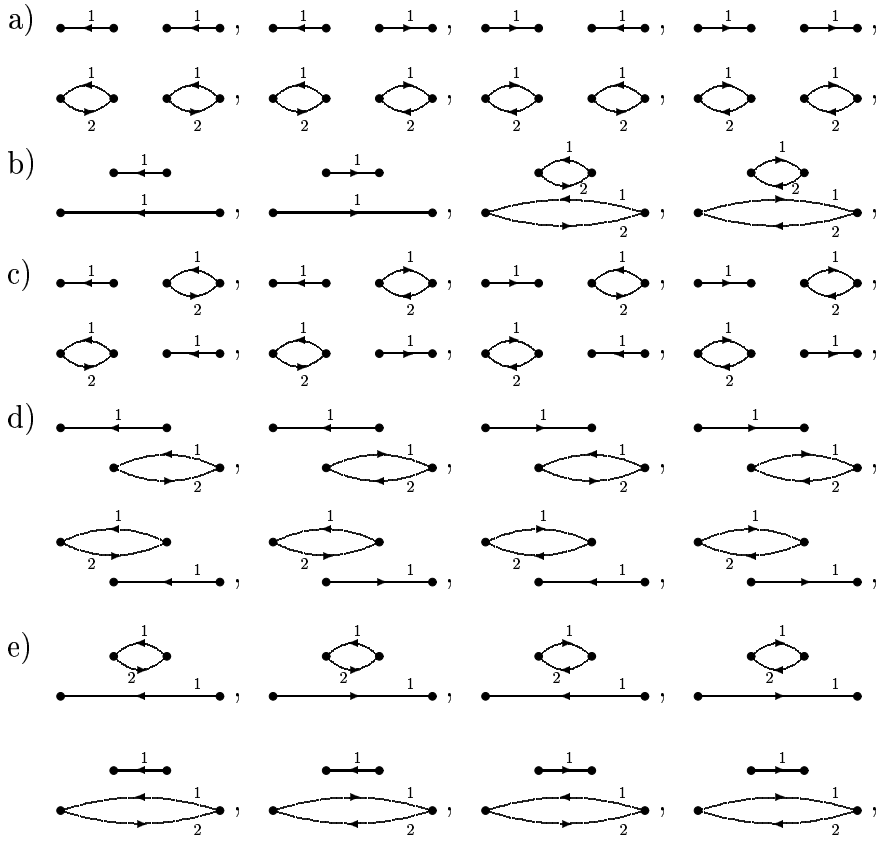

Figure 4.1: All λ^4 diagrams. Diagrams in a) and b) involve vertices only from a single resonance and so belong to the single resonance part of the dynamics. Diagrams in c), d) and e) involving vertices from both resonances correspond to the interference part of the dynamics.

transitions are:

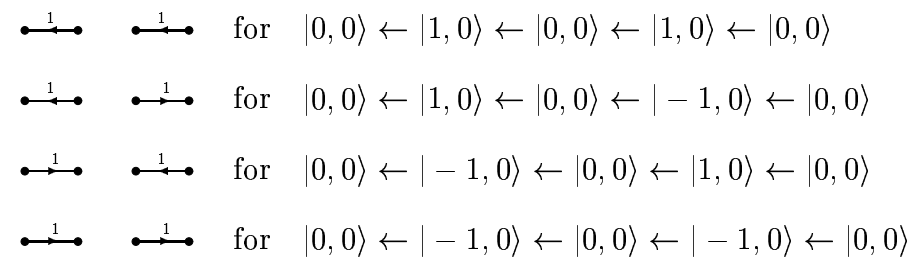

$$\begin{aligned}
&\text{for} \quad |0,0\rangle \leftarrow |1,0\rangle \leftarrow |0,0\rangle \leftarrow |1,0\rangle \leftarrow |0,0\rangle \\
&\text{for} \quad |0,0\rangle \leftarrow |1,0\rangle \leftarrow |0,0\rangle \leftarrow |-1,0\rangle \leftarrow |0,0\rangle \\
&\text{for} \quad |0,0\rangle \leftarrow |-1,0\rangle \leftarrow |0,0\rangle \leftarrow |1,0\rangle \leftarrow |0,0\rangle \\
&\text{for} \quad |0,0\rangle \leftarrow |-1,0\rangle \leftarrow |0,0\rangle \leftarrow |-1,0\rangle \leftarrow |0,0\rangle
\end{aligned} \tag{4.13}$$

where we have to read the transitions from right to left. Note that these diagrams are constructed from a succession of sub-diagrams called "diagonal fragments" [17], It is well known that they give the most secular time dependence in the case of $\lambda^2 t$-approximation for the large Poincaré system as discussed in Appendix B.

By following the diagrammatic rules stated in Appendix C, the corresponding expression of $\langle A(\vec{J})\rangle_t^{(4)}$ for the sum of these four diagrams(transitions) is given by

$$\begin{aligned}
&\frac{\lambda^4}{2^5\pi i}\int d^2J A(\vec{J})\int_C dz \frac{e^{-izt}}{z^3}\sum_{n,n'=\pm 1}\partial_1\frac{1}{nJ_1-z}\partial_1^2\frac{1}{n'J_1-z}\partial_1\rho_{\vec{0}}(\vec{J},0) \\
=&\frac{\lambda^4}{2^3\pi i}\int d^2J A(\vec{J})\int_C dz \frac{e^{-izt}}{z}\partial_1\frac{1}{J_1^2-z^2}\partial_1^2\frac{1}{J_1^2-z^2}\partial_1\rho_{\vec{0}}(\vec{J},0)
\end{aligned} \tag{4.14}$$

Now we apply the procedure presented in the last section to evaluate the most secular effect by calculating the residues,

$$\begin{aligned}
&\frac{\lambda^4}{2^3\pi i}(2\pi i)^2 \operatorname*{Res}_{z=i0}\operatorname*{Res}_{J_1=z}\left[\int dJ_2 \frac{e^{-izt}}{z}A(\vec{J})\partial_1\frac{1}{J_1^2-z^2}\partial_1^2\frac{1}{J_1^2-z^2}\partial_1\rho_{\vec{0}}(\vec{J},0)\right] \\
\sim&\frac{\lambda^4\pi i}{16}\operatorname*{Res}_{z=i0}\left[\frac{e^{-izt}}{z^6}\int dJ_2(\partial_1 A(\vec{J}))(\partial_1\rho_{\vec{0}}(\vec{J},0))\Big|_{J_1=z}\right]
\end{aligned} \tag{4.15}$$

As a result, the sixth order pole $1/z^6$ gives the most secular effect of (4.15) as

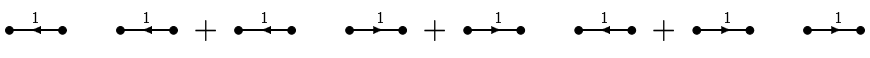

$$\sim \frac{\lambda^4 t^5 \pi}{(16)(5!)} \int dJ_2 (\partial_1 A(\vec{J}))(\partial_1 \rho_{\vec{0}}(\vec{J},0))\Big|_{J_1=0} \tag{4.16}$$

Therefore, a new secular time dependence $\lambda^4 t^5$ appears in the small Poincaré system.

Recall that the fourth order contribution in the large Poincaré system gives us $(\lambda^2 t)^2$ as the most secular effect, which is a weaker secular effect than that of the small Poincaré system. It is because the wave vector $\{n, n'\}$ in (4.14) is continuous for the large Poincaré system so that the intermediate propagators $(nJ_1 - z)^{-1}$ and $(n'J_1 - z)^{-1}$ in the first line of (4.14) can not generate new singularities at $z = 0$ after the integration over the continuous wave vector $\{n, n'\}$. For the present case of small Poincaré system, n and n' are discrete variables. Therefore the interference between the two propagators generates an extra singularity of z^{-3} in addition to the factor z^{-3} in front of the summation sign in (4.14). As a result, we have a stronger secular effect in the small Poincaré system.

However, If we look at the four diagrams in (4.13) we just considered more carefully, one can find that not all of them are as secular as $\lambda^4 t^5$. For example, the cross terms with $n = 1, n' = -1$ ( ) and $n = -1, n' = 1$ (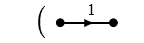) in (4.14) give rise to the sixth order pole in z

$$\frac{1}{z^3} \underset{J_1=z}{\text{Res}} \left[\frac{1}{J_1 + z} \partial_1^2 \frac{1}{J_1 - z} \right] \sim \frac{1}{z^3} \underset{J_1=z}{\text{Res}} \left[\frac{1}{J_1 - z} \partial_1^2 \frac{1}{J_1 + z} \right] \sim \frac{1}{z^6} \tag{4.17}$$

The most secular time dependence in (4.17) is therefore given by $\lambda^4 t^5$ after taking the residue in z.

On the other hand, the terms with $n = 1, n' = 1$ (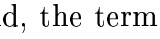) and $n = -1, n' = -1$ (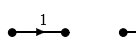) give

$$\frac{1}{z^3}\underset{J_1=z}{\text{Res}}\left[\frac{1}{J_1+z}\partial_1^2\frac{1}{J_1+z}\right] = \frac{1}{z^3}\underset{J_1=z}{\text{Res}}\left[\frac{1}{J_1-z}\partial_1^2\frac{1}{J_1-z}\right] = 0 \tag{4.18}$$

and therefore the time dependence of these terms are less secular than $\lambda^4 t^5$. In fact, if all poles on the complex-J_1 plane are above or below the real-J_1 axis, the residue of a general transition vanishes as in (4.18), and the term is less secular.

Similar results can be found for the four diagrams listed in the second line of Figure 4.1a) which come from the resonance at $J_1 = \omega_2$. They are given by

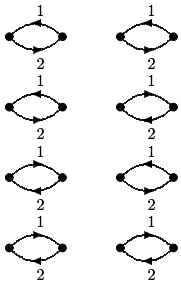 $< \lambda^4 t^5$ for $|0,0\rangle \leftarrow |1,-1\rangle \leftarrow |0,0\rangle \leftarrow |1,-1\rangle \leftarrow |0,0\rangle$

 $\sim \lambda^4 t^5$ for $|0,0\rangle \leftarrow |1,-1\rangle \leftarrow |0,0\rangle \leftarrow |-1,1\rangle \leftarrow |0,0\rangle$

 $\sim \lambda^4 t^5$ for $|0,0\rangle \leftarrow |-1,1\rangle \leftarrow |0,0\rangle \leftarrow |1,-1\rangle \leftarrow |0,0\rangle$

 $< \lambda^4 t^5$ for $|0,0\rangle \leftarrow |-1,1\rangle \leftarrow |0,0\rangle \leftarrow |-1,1\rangle \leftarrow |0,0\rangle$ (4.19)

where $< \lambda^4 t^5$ means that the diagram is less divergent than $\lambda^4 t^5$. The transitions(diagrams) in the first and last line of (4.19) are less secular again due to the fact that the poles on the complex-J_1 plane all lie either above or below the real-J_1 axis.

Now we turn to the diagrams in Figure 4.1b). From now on, we will represent all transitions by diagrams and will not write out the explicit form of the intermediate states unless it is necessary to do so. Again, by using the new procedure, one can find that all the four diagrams in figure 4.1b) are less secular than $\lambda^4 t^5$. For example, we have

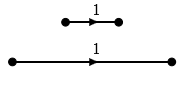

$$\sim -\frac{\lambda^4}{2^3\pi i}(2\pi i)^2 \operatorname*{Res}_{z=i0} \operatorname*{Res}_{J_1=z}\Bigg[\int dJ_2 \frac{e^{-izt}}{z^2} A(\vec{J})\partial_1 \frac{1}{-J_1-z}\partial_1 \frac{1}{-2J_1-z} \times \partial_1 \frac{1}{-J_1-z}\partial_{12}\rho_{\vec{0}}(\vec{J},0)\Bigg] < \lambda^4 t^5 \tag{4.20}$$

since all poles are located below the real-J_1 axis.

From the above exercises, we are now ready to summarize the rules for selecting the most secular diagrams for the single resonance part of our system:

1. The diagrams of the single resonance part must consist of only one type of vertices from a single resonance, i.e. single resonance diagrams consist of vertices either from Figure C.2a) or Figure C.2b).

2. If all poles of the propagators $1/(n_1^{(i)}J_1+n_2^{(i)}\omega_2-z)$ in a diagram lie on the upper or lower half complex-J_1 plane in the asymptotic limit $z \to i0^+$, the diagram is less secular (i.e. transitions with $n_1^{(i)} \geq 0$ or $n_1^{(i)} \leq 0$ for all i are less secular) due to the vanishing of the residue as in (4.18). In the language of diagram representation, it means that the directed lines with label 1 of a most secular diagram must point in both directions.

3. Since the directed lines with label 1 of a most secular diagram can point in both directions, there must be some intermediate states $|\vec{n}^{(i)}\rangle$ with $n_1^{(i)} = 0$ for some $1 \leq i \leq k-1$. In other words, the most secular diagrams for the single resonance part must be "disconnected" except for the second order diagrams. A disconnected diagram is diagram which can be broken into several connected sub-diagrams, e.g. diagrams in Figure 4.1a) are disconnected and diagrams in Figure 4.1b) are connected. However, within these connected sub-diagrams, all directed lines with label 1 point in the same direction in order for the whole diagram to be most secular.

4.2.4 Higher Order Contributions

By using the diagrammatic representation and the rules stated in the last section , we list the most secular diagrams of sixth order and their most

secular time dependence

$$\langle A(\vec{J})\rangle_t^{(6)}$$

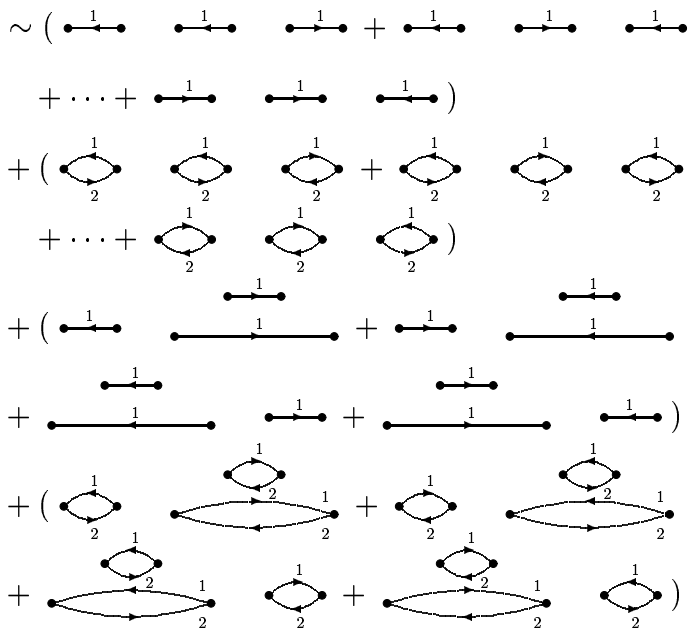

$$\sim \lambda^6 t^9 \qquad (4.21)$$

At this stage, it is interested to compare this result (4.21) with the sixth order contribution in the large Poincaré system. For the large Poincaré system, it is well known that the most secular effect $(\lambda^2 t)^3$ in sixth order comes from the diagrams that consist of three irreducible diagonal transitions. Here, irreducible diagonal transition means that there always appears some non-vanishing lines in the intermediate states. For example, the first term on the right-hand side of (4.21), i.e. 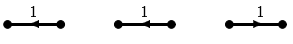 , consists of three irreducible diagonal transitions. On the other hand, the last term on the right hand side of (4.21) consists of two irreducible diagonal transitions. For the large Poincaré system. the first term gives $\lambda^6 t^3$ secular contribution, while the last term gives $\lambda^6 t^2$

secular contribution. In contrast, we obtain $\lambda^6 t^9$ secular contributions from all diagrams displayed in (4.21) for the small Poincaré system.

One can repeat the similar calculation for the most secular contribution with arbitrary power of λ. Since the calculation is tedious even it is straightforward, we only display the result and the estimation will be discussed in Appendix D. The most secular effect for the single resonance part of our small Poincaré system is given by

$$\begin{aligned}
&\langle A(\vec{J})\rangle_t \\
&\sim \int d^2J A(\vec{J})\rho_{\vec{0}}(\vec{J},0) \\
&\quad + \left[-\frac{\lambda^2 t\pi}{2} + \frac{\lambda^4 t^5 \pi}{(16)(5!)} + \cdots + \frac{(-1)^m \lambda^{2m} t^{4m-3}\pi a_m}{2^{2m-1}(4m-3)!} + \cdots\right] \\
&\quad \times \int dJ_2 \left[(\partial_1 A(\vec{J}))(\partial_1 \rho_{\vec{0}}(\vec{J},0))\Big|_{J_1=0} + (\partial_{12} A(\vec{J}))(\partial_{12}\rho_{\vec{0}}(\vec{J},0))\Big|_{J_1=\omega_2}\right] \\
&= \int d^2J A(\vec{J})\rho_{\vec{0}}(\vec{J},0) + \lambda^{3/2}\pi \sum_{m=1}^{\infty} \frac{(-1)^m (\sqrt{\lambda}t)^{4m-3} a_m}{2^{2m-1}(4m-3)!} \\
&\quad \times \int dJ_2 \left[(\partial_1 A(\vec{J}))(\partial_1 \rho_{\vec{0}}(\vec{J},0))\Big|_{J_1=0} + (\partial_{12} A(\vec{J}))(\partial_{12}\rho_{\vec{0}}(\vec{J},0))\Big|_{J_1=\omega_2}\right]
\end{aligned} \tag{4.22}$$

where a_m is determined by the residues

$$\begin{aligned}
&\sum_{\{\vec{n}\}}{}' \operatorname*{Res}_{J_1=\{\xi\}} \left[\frac{1}{\vec{n}^{(2m-1)}\cdot\vec{\Omega}-z}\partial_1 \frac{1}{\vec{n}^{(2m-2)}\cdot\vec{\Omega}-z}\partial_1 \cdots \partial_1 \frac{1}{\vec{n}^{(1)}\cdot\vec{\Omega}-z}\right] \\
&\quad = \frac{a_m}{z^{4m-4}}
\end{aligned} \tag{4.23}$$

where $\Sigma'_{\{\vec{n}\}}$ means summation over the most secular transitions, and $\{\xi\}$ is the set of poles of the propagators $(\vec{n}^{(i)}\cdot\vec{\Omega}-z)^{-1}$ on the upper half complex-J_1 plane.

Therefore, we obtain a stronger secular contribution of $\lambda^{3/2}(\sqrt{\lambda}t)^{4m-3}$ for the small Poincaré system instead of the $(\lambda^2 t)^m$ contribution in the large Poincaré system. Since the secular contributions come from the resonance effects, this implies that the small Poincaré system has a stronger resonance effect than the large Poincaré system. The expression (4.22) gives a predominant contribution to $\langle A(\vec{J})\rangle_t$ in the time scale of order $t \sim 1/\sqrt{\lambda}$ for $\lambda \ll 1$.

4.2.5 Comparison to the Numerical Simulation

In order to compare our result to the numerical simulation, We consider the time evolution of the expectation value $\langle J_1\rangle_t$ with the normalized initial distribution function

$$\begin{aligned}\rho(\vec{J},\vec{\theta},t=0) &= \rho_{\vec{0}}(\vec{J},t=0)/(2\pi)^2 \\ &= (\sigma\sqrt{\pi})^{-1}\exp(-(J_1-J_{10})^2/\sigma^2)\delta(J_2-J_{20})\end{aligned} \tag{4.24}$$

where $\sigma > 0$, $\infty > J_{10} > -\infty$ and $J_{20} > 0$ are constants. This choice of the initial distribution function simplifies our numerical simulation (especially in the case of the interference part discussed in the next chapter) since the phase space integration over J_2 can be performed analytically due to the delta function $\delta(J_2 - J_{20})$.

In Figure 4.2, we show the comparison between the theoretical prediction (4.22) and the numerical simulation in the time scale $t \sim 1/\sqrt{\lambda}$ with $\lambda = 0.01$, $\sigma = 1.0$, $J_{10} = 0.3$ and $J_{20} = 1.0$, where the most secular series (4.22) is calculated up to the order of λ^{16}. The numerical result is obtained by solving the equation of motion (2.3) with an ensemble of trajectories distributed

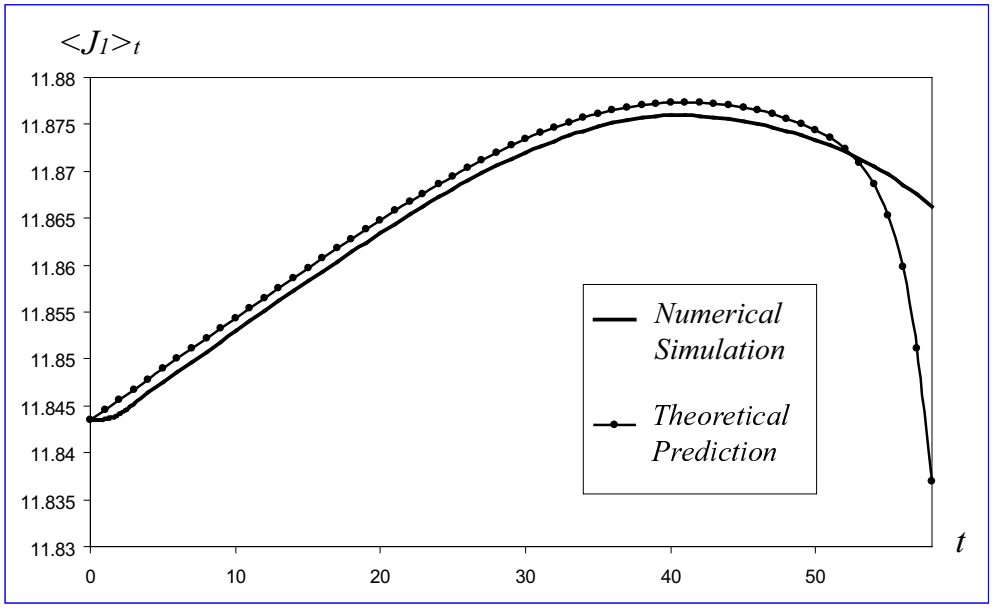

Figure 4.2: Comparison of the theoretical prediction for the single resonance part (4.22) to the numerical simulation of the full dynamics. We show the time evolution of the expectation value $\langle J_1 \rangle_t$ with initial distribution function $\rho(\vec{J}, \vec{\theta}, t = 0) = (\sigma\sqrt{\pi})^{-1} \exp(-(J_1 - J_{10})^2/\sigma^2)\delta(J_2 - J_{20})$ where $\sigma = 1.0$, $J_{10} = 0.3$, and $J_{20} = 1.0$. The coupling constant is $\lambda = 0.01$ and $\omega_2 = 0.8$.

according to our choice of the initial probability distribution (4.24).

From Figure 4.2, we see that the most secular effect of the single resonance part gives a good approximation to the full dynamics up to $t \approx 5/\sqrt{\lambda} = 50$. The big deviation between the theoretical prediction and the numerical simulation for $t > 5/\sqrt{\lambda}$ is due to the fact that the most secular series is truncated at the order of λ^{16}. On the other hand, we observe that the full dynamics near $t = 0$ (the flat part of the numerical curve) is different from the most secular effect ($\sim \lambda^2 t$ see (4.22)) and so comes from the less secular effects.

The full dynamics of the expectation value of a general observable $\langle A(\vec{J})\rangle_t$ near $t = 0$ can be understood by Taylor expanding $\langle A(\vec{J})\rangle_t$ around $t = 0$. In particular, the first derivative of $\langle A(\vec{J})\rangle_t$ evaluated at $t = 0$ is given by

$$\begin{aligned}\left.\frac{d\langle A(\vec{J})\rangle_t}{dt}\right|_{t=0} &= \left.\frac{d}{dt}\left(\int d^2J d^2\theta A(\vec{J})\rho(\vec{J},\vec{\theta},t)\right)\right|_{t=0} \\ &= \left.\frac{d}{dt}\left(\int d^2J d^2\theta A(\vec{J}) e^{-iLt}\rho(\vec{J},t=0)\right)\right|_{t=0} \\ &= -i\int d^2J d^2\theta A(\vec{J}) L\rho(\vec{J},t=0)\end{aligned} \tag{4.25}$$

where we have used the fact that the initial distribution function we considered is independent of the angle variables. The operator $\exp(-iLt)$ is the time evolution operator with L the Liouville operator given in (3.3). We then have

$$\left.\frac{d\langle A(\vec{J})\rangle_t}{dt}\right|_{t=0} = -i\int d^2J d^2\theta A(\vec{J})(L_0 + \lambda L)\rho(\vec{J},t=0) = 0 \tag{4.26}$$

since $L_0\rho(\vec{J}, t=0) = 0$ and $\int d^2\theta(\delta L)\rho(\vec{J}, t=0) = 0$ by using (3.4) and (3.5). Therefore the numerical curve of the expectation value in Figure 4.2 must be flat at $t = 0$. On the other hand, since

$$\begin{aligned}
\left.\frac{d^2\langle A(\vec{J})\rangle_t}{dt^2}\right|_{t=0} &= \left.\frac{d^2}{dt^2}\left(\int d^2Jd^2\theta A(\vec{J})e^{-iLt}\rho(\vec{J}, t=0)\right)\right|_{t=0} \\
&= -\int d^2Jd^2\theta A(\vec{J})L^2\rho(\vec{J}, t=0) \\
&= -\int d^2Jd^2\theta A(\vec{J})(\delta L)^2\rho(\vec{J}, t=0) \\
&\neq 0
\end{aligned} \tag{4.27}$$

the full dynamics of the expectation value around $t = 0$ is given by

$$\langle A(\vec{J})\rangle_t = \langle A(\vec{J})\rangle_{t=0} + (t^2/2)(d^2/dt^2)(\langle A(\vec{J})\rangle|_{t=0}) + \cdots \tag{4.28}$$

in contrast to the most secular effect (4.22) with $\langle A(\vec{J})\rangle_t \sim \langle A(\vec{J})\rangle_{t=0} + O(t)$ which breaks the time symmetry as in the case of the large Poincaré system [17].

Chapter 5

Interference between Resonances

5.1 Motivation

We have seen from the discussion in Chapter 2 that non-integrability of our system comes from the appearance of many resonance terms due to the interference of the resonance interactions in the Hamiltonian. It is the objective in this chapter to consider the interference between the resonances and discuss its implications.

Since the interference diagrams first appear in fourth order, we will look at the fourth order contributions in Section 5.2, and evaluate their secular effect by using the same procedure we presented in the last chapter. In fourth order, there appears new poles at $z = \pm\omega_2/2$ besides the one at $z = 0$. These new poles are related to the higher harmonics in the non-linear system. We will show that these new singularities give rise to the secular effect in powers of t as well as oscillation corresponding to the higher order resonances. Higher order contributions will be treated in Section 5.3.

For the weakly-coupled case ($\omega_2 \gg \sqrt{\lambda}$) in which the separation between the two primary resonances is big compared to the width of these separatrices, one may expect that the interference part only gives a small correction

to the single resonance effect discussed in the previous chapter. However, the consistent estimation of the interference effect is so important no matter how small it is, as this is the first non-trivial correction that comes from the non-integrability of the system. In the following discussion, we will restrict our consideration to this weakly-coupled case.

For the strongly-coupled case where we have $\omega_2 \sim \sqrt{\lambda}$, the interference effect starts to be dominant as compared with the single resonance part. One can no longer treat the interference part as a correction to the secular effect from the single resonance part discussed in the last chapter. As we will show, the condition $\omega_2 \sim \sqrt{\lambda}$ leads to the same resonance overlapping condition that has been discussed previously by Chirikov [5] to describe the onset of global chaos in non-integrable systems from the trajectory point of view. It is interesting to obtain the same criterion by analyzing the secular effect on the level of ensemble theory.

We will compare our results with the numerical simulations in Section 5.5.

5.2 Fourth Order Contribution

According to the discussion in Section 4.2.3, one can see that eight interference diagrams shown in Figure 4.1c)-e) can be most secular. It is because they give vanishing lines with label 1 in the intermediate state so that the residue does not vanish. These most secular diagrams for the interference part is shown in Figure 5.1.

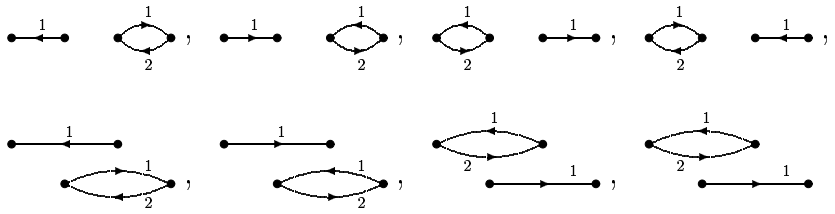

Figure 5.1: The most secular λ^4 interference diagrams

Let us first consider the diagram 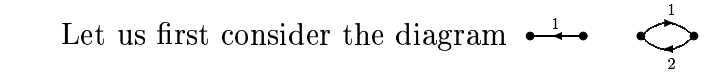 in Figure 5.1. According to Appendix C, its mathematical expression is

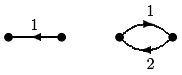

$$
\begin{aligned}
&= \frac{-\lambda^4}{2\pi i}\int d^2J A(\vec{J})\int_C dz e^{-izt}\frac{1}{z^2}\langle\vec{0}|\delta L|1,0\rangle\frac{1}{J_1-z}\langle 1,0|\delta L|\vec{0}\rangle \\
&\quad\times\frac{1}{-z}\langle\vec{0}|\delta L|-1,1\rangle\frac{1}{-J_1+\omega_2-z}\langle -1,1|\delta L|\vec{0}\rangle\rho_{\vec{0}}(\vec{J},0) \\
&= \frac{\lambda^4}{2^5\pi i}\int d^2J\int_C dz\frac{e^{-izt}}{z^3}A(\vec{J})\partial_1\frac{1}{J_1-z}\partial_1\partial_{12}\frac{1}{-J_1+\omega_2-z}\partial_{12}\rho_{\vec{0}}(\vec{J},0)
\end{aligned}
\tag{5.1}
$$

where we have used (4.2) and (4.3) for the matrix elements of our system in the second line. For $A(\vec{J}) = J_1$ and $\rho_{\vec{0}}(\vec{J},0) = \rho_1(J_1)\delta(J_2 - J_{20})$ with $\rho_1(J_1) = (4\pi^{3/2}/\sigma)\exp(-(J_1-J_{10})^2/\sigma^2)$ as in the last chapter, we have

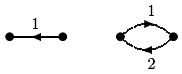

$$
= \frac{-\lambda^4}{2^5\pi i}\int dJ_1\int_C dz\frac{e^{-izt}}{z^3}\frac{1}{J_1-z}\partial_1^2\frac{1}{-J_1+\omega_2-z}\partial_1\rho_1(J_1)
\tag{5.2}
$$

Note that in the above equation, the propagators $(J_1-z)^{-1}$ and $(-J_1+\omega_2-z)^{-1}$ come from the transitions due to the two resonances at $J_1 = 0$ and $J_1 = \omega_2$ respectively. Now, we apply the procedure discussed in the last chapter to find the secular effect caused by the interference between these resonances by

evaluating the residue of the poles of J_1 in the upper half complex-J_1 plane. We have

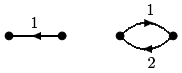

$$\begin{aligned}
&\sim \frac{-\lambda^4}{2^4}\int_C dz \frac{e^{-izt}}{z^3}\operatorname*{Res}_{J_1=z}\left[\frac{1}{J_1-z}\partial_1^2\frac{1}{-J_1+\omega_2-z}\partial_1\rho_1(J_1)\right] \\
&\sim \frac{-\lambda^4}{2^4}\int_C dz \frac{e^{-izt}}{z^3}\left[\frac{2\rho_1'(J_1)}{(\omega_2-2z)^3}+\frac{2\rho_1''(J_1)}{(\omega_2-2z)^2}+\frac{\rho_1^{(3)}(J_1)}{\omega_2-2z}\right]\Bigg|_{J_1=z}
\end{aligned} \tag{5.3}$$

A new pole appears at $z=\omega_2/2$ in contrast to the case of single resonance in which we only have a pole at $z=0$ (see for example (4.17) and (4.18)). The new pole comes from the interference between the propagators $(J_1-z)^{-1}$ and $(-J_1+\omega_2-z)^{-1}$. To obtain the secular effect of these poles, we evaluate the contour integration of z by taking the residue in z at the poles $z=0$ and $z=\omega_2/2$ as

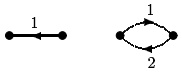

$$\sim \frac{-\lambda^4\pi i}{2^3}\operatorname*{Res}_{z=0,\,\omega_2/2}\left[\frac{e^{-izt}}{z^3}\left(\frac{2\rho_1'(J_1)}{(\omega_2-2z)^3}+\frac{2\rho_1''(J_1)}{(\omega_2-2z)^2}+\frac{\rho_1^{(3)}(J_1)}{\omega_2-2z}\right)\Bigg|_{J_1=z}\right] \tag{5.4}$$

The residue of the pole at $z=0$ gives rise to the secular effect in powers of t as

$$\begin{aligned}
&\frac{-\lambda^4\pi i}{2^3}\operatorname*{Res}_{z=0}\left[\frac{e^{-izt}}{z^3}\left(\frac{2\rho_1'(J_1)}{(\omega_2-2z)^3}+\frac{2\rho_1''(J_1)}{(\omega_2-2z)^2}+\frac{\rho_1^{(3)}(J_1)}{\omega_2-2z}\right)\Bigg|_{J_1=z}\right] \\
&\sim 2\pi\lambda^4\left[it^2\left(\frac{\rho_1'(J_1)}{16\omega_2^3}+\frac{\rho_1''(J_1)}{16\omega_2^2}+\frac{\rho_1^{(3)}(J_1)}{32\omega_2}\right)\right. \\
&\qquad \left.-t\left(\frac{3\rho_1'(J_1)}{4\omega_2^4}+\frac{5\rho_1''(J_1)}{8\omega_2^3}+\frac{\rho_1^{(3)}(J_1)}{4\omega_2^2}+\frac{\rho_1^{(4)}(J_1)}{16\omega_2}\right)+O(t^0)\right]\Bigg|_{J_1=0}
\end{aligned} \tag{5.5}$$

Similarly, the secular terms corresponding to the residue of the pole at

$z = \omega_2/2$ is given by

$$\begin{aligned}
&\frac{-\lambda^4\pi i}{2^3}\operatorname*{Res}_{z=\omega_2/2}\left[\frac{e^{-izt}}{z^3}\left(\frac{2\rho_1'(J_1)}{(\omega_2-2z)^3}+\frac{2\rho_1''(J_1)}{(\omega_2-2z)^2}+\frac{\rho_1^{(3)}(J_1)}{\omega_2-2z}\right)\Big|_{J_1=z}\right] \\
&\sim 2\pi i\lambda^4 e^{-i\omega_2 t/2}\left[-\frac{t^2\rho_1'(J_1)}{16\omega_2^3}+it\left(\frac{3\rho_1'(J_1)}{4\omega_2^4}+\frac{\rho_1''(J_1)}{8\omega_2^4}\right)+O(t^0)\right]\Big|_{J_1=\omega_2/2}
\end{aligned} \tag{5.6}$$

In (5.5) and (5.6), we have included the next most secular effect of order $\lambda^4 t$ since we will see later that all terms proportional to $\lambda^4 t^2$ cancel out after the summation over the contribution from all the eight diagrams in Figure 5.1. Therefore, by keeping only the secular contribution of order $\lambda^4 t$ in (5.5) and (5.6), the most secular effect is given by

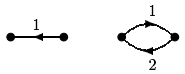

$$\begin{aligned}
&\sim -\pi\lambda^4 t\left(\frac{3\rho_1'(J_1)}{2\omega_2^4}+\frac{5\rho_1''(J_1)}{4\omega_2^3}+\frac{\rho_1^{(3)}(J_1)}{4\omega_2^2}+\frac{\rho_1^{(4)}(J_1)}{8\omega_2}\right)\Big|_{J_1=0} \\
&-\pi i\lambda^4 t e^{-i\omega_2 t/2}\left(\frac{3\rho_1'(J_1)}{2\omega_2^4}+\frac{\rho_1''(J_1)}{4\omega_2^4}\right)\Big|_{J_1=\omega_2/2}
\end{aligned} \tag{5.7}$$

Therefore, the evaluation of the resonance interference effect gives rise to two types of secular effect. The singularity at $z = 0$ gives the secular behavior of $\lambda^4 t$ in (5.5) while the pole at $z = \omega_2/2$ leads to the secular effect $\lambda^4 t \exp(-i\omega_2 t/2)$ in (5.6).

The secular effect with oscillation $\lambda^4 t \exp(-i\omega_2 t/2)$ can be easily related to the period two solution associated with the secondary resonance located at $J_1 = \omega_2/2$ for our system. This period two solution (with the period two fixed points at $\{J_1 = \omega_2/2,\, \theta_1 = 0\}$ and $\{J_1 = \omega_2/2,\, \theta_1 = \pi\}$) can be seen from the stroboscopic plot in Figure 2.1a) discussed in Section 2.2. It comes from the

particular solution ($J_1 = \omega_2/2$, $\theta_1 = \omega_2 t/2$, $\theta_2 = \omega_2 t$) of the equation of motion (2.3) with $t = 2n\pi/\omega_2$, $n = 1, 2, \cdots$. The angular frequency $\omega_2/2$ of the angle variable θ_1 gives the oscillation $\exp(-i\omega_2 t/2)$ in the secular effect. However in the trajectory approach, it is generally not easy to find such higher periodic solutions of the non-integrable systems. By evaluating the secular terms in the ensemble approach, one can automatically take into account the contributions from the resonance effects of these higher periodic motions.

Similar results can be obtained for the other diagrams in Figure 5.1. For example, the secular effect of the last diagram in Figure 5.1 can be found by the procedure parallel to the above discussion as

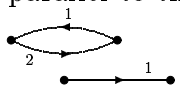

$$\begin{aligned} &\sim \pi\lambda^4 t\left(\frac{\rho_1'(J_1)}{4\omega_2^4} - \frac{\rho_1''(J_1)}{4\omega_2^3} + \frac{\rho_1^{(3)}(J_1)}{8\omega_2^2}\right)\Bigg|_{J_1=\omega_2} \\ &+ \pi\lambda^4 t e^{i\omega_2 t/2}\left(\frac{\rho_1'(J_1)}{2\omega_2^4} - \frac{\rho_1''(J_1)}{4\omega_2^3}\right)\Bigg|_{J_1=\omega_2/2} \end{aligned} \tag{5.8}$$

where we have again kept only the secular terms proportional to $\lambda^4 t$.

After summing the contributions from all the diagrams in Figure 5.1, the $\lambda^4 t^2$ terms cancel out and we obtain the fourth order most secular effect for the interference part as

$$\begin{aligned} &\sim -\lambda^4 t\pi\left(\frac{5\rho_1'(J_1)}{2\omega_2^4} + \frac{5\rho_1''(J_1)}{4\omega_2^3} + \frac{3\rho_1^{(3)}(J_1)}{8\omega_2^2} + \frac{\rho_1^{(4)}(J_1)}{8\omega_2}\right)\Bigg|_{J_1=0} \\ &- \lambda^4 t\pi\left(\frac{5\rho_1'(J_1)}{2\omega_2^4} - \frac{5\rho_1''(J_1)}{4\omega_2^3} + \frac{3\rho_1^{(3)}(J_1)}{8\omega_2^2} - \frac{\rho_1^{(4)}(J_1)}{8\omega_2}\right)\Bigg|_{J_1=\omega_2} \\ &- \frac{2\lambda^4 t\pi\rho_1'(J_1)}{\omega_2^4}(e^{i\omega_2 t/2} + e^{-i\omega_2 t/2})\Bigg|_{J_1=\omega_2/2} \end{aligned} \tag{5.9}$$

Let us now compare (5.9) with the most secular effect $\lambda^4 t^5$ obtained in (4.22) for the fourth order single resonance contribution in the last chapter. The ratio of (5.9) to (4.22) is given as

$$\left(\frac{1}{\omega_2 t}\right)^4 \sim \left(\frac{\sqrt{\lambda}}{\omega_2}\right)^4 \tag{5.10}$$

for $t \sim 1/\sqrt{\lambda}$. Hence (5.9) is a small correction for the weakly-coupled case ($\omega_2 \gg \sqrt{\lambda}$) as mentioned before.

5.3 Higher Order Contributions

Using the same procedure, we can calculate the most secular effect from the higher order contributions. We find that new poles at $z = \pm\omega_2$ appear in the sixth order calculation and again lead to secular effect with oscillation. With $A(\vec{J}) = J_1$ and $\rho_{\vec{0}}(\vec{J}, 0) = \rho_1(J_1)\delta(J_2 - J_{20})$ as before, we have

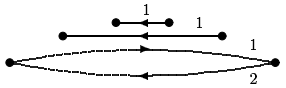

$$\sim \lambda^6 t^7 e^{-i\omega_2 t} \rho_1'(J_1 = 0)/\omega_2^2 \tag{5.11}$$

where this most secular effect is obtained by taking the residue of the pole at $z = \omega_2$. Similarly, we have

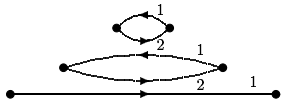

$$\sim \lambda^6 t^7 e^{i\omega_2 t} \rho_1'(J_1 = \omega_2)/\omega_2^2 \tag{5.12}$$

from the pole $z = -\omega_2$.

Since the number of most secular interference diagrams increases rapidly as the order of λ increases in the approximation, we do not show all the most

secular diagrams here but just write down the results for the sixth order contributions as

$$\sim \lambda^6 t^7 (e^{i\omega_2 t} + e^{-i\omega_2 t})(\rho_1'(J_1 = 0) + \rho_1'(J_1 = \omega_2))/\omega_2^2 \tag{5.13}$$

The eighth order contributions have been calculated similarly. We again find secular effect with oscillation $\sim \lambda^8 t^{11} \exp(\pm i\omega_2 t)/\omega_2^2$. In Figure 5.2, We show the secular effects of the λ^4, λ^6 and λ^8 contributions with $\sigma = 1.0$, $J_{10} = 0.3$, $J_{20} = 1.0$, $\omega_2 = 0.8$ and the coupling constant $\lambda = 0.01$. We see that the λ^4 contribution with oscillation frequency $\omega_2/2$ is dominant in the time scale of $t \sim 1/\sqrt{\lambda}$ for the interference part.

5.4 Resonance Overlapping Condition

Now, we compare the most secular effect of the interference part to that of the single resonance part discussed in the last chapter. From (5.10), We see that the contribution of the interference part is comparable to the single resonance part when $\omega_2 \sim \sqrt{\lambda}$. In this situation, the interference part is no longer a small correction to the single resonance part. It is interesting to see that the condition $\omega_2 \sim \sqrt{\lambda}$ obtained by analyzing the secular effects on the level of ensemble is consistent with the Chirikov overlapping condition [5] for the onset of global chaos. Since the interference part comes from the non-integrability of the system, we then see that there is a close relation between non-integrability and chaos in our system.

On the other hand, If one also keeps the less secular effects in the

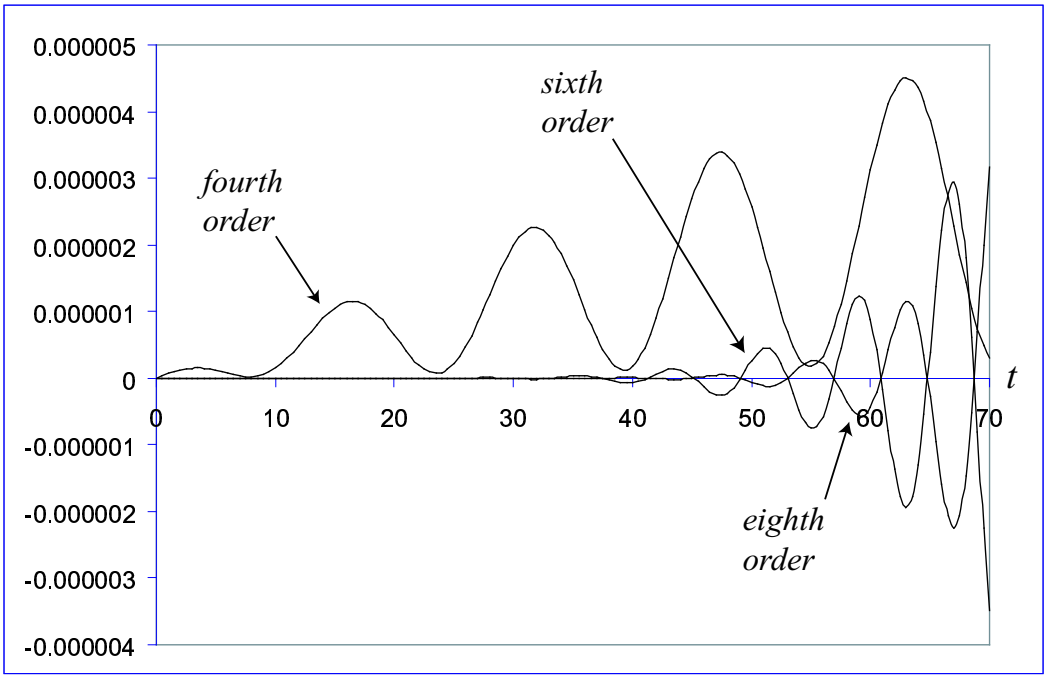

Figure 5.2: The λ^4, λ^6 and λ^8 order contributions of the most secular effect for the interference part.

calculation of the higher order contributions in Section 5.3, say for example in λ^6 order, there appears the less secular time dependences ($\lambda^6 t^6/\omega_2^3$, $\lambda^6 t^5/\omega_2^4$, $\lambda^6 t^4/\omega_2^5, \cdots$) corresponding to the higher order resonances. These less secular contributions are also comparable to the most secular effect $\lambda^6 t^9$ of the single resonance part (see (4.22)) if $\omega_2 \sim \sqrt{\lambda}$, i.e.

$$\lambda^6 t^9 \sim \lambda^6 t^7/\omega_2^2 \sim \lambda^6 t^6/\omega_2^3 \sim \lambda^6 t^5/\omega_2^4 \sim \cdots \tag{5.14}$$

when $\omega_2 \sim \sqrt{\lambda}$ for $t \sim 1/\sqrt{\lambda}$. In here, $\lambda^6 t^7/\omega_2^2$ is the most secular effect of the λ^6 order contribution of the interference part (see (5.13)). Therefore, when the resonances strongly couple to each others, $\omega_2 \sim \sqrt{\lambda}$, one can no longer keep only the most secular terms in the interference case, and the less secular effects from the higher order resonances must be taken into account. The study of the strongly-coupled case and the less secular effects from the higher order resonance effects will be considered in the future work.

5.5 Comparison to the Numerical Simulation

In order to compare our theoretical prediction in Section 5.2 and 5.3 to the numerical simulation, we need to extract the contribution of interference part from the full dynamics. Recall from (4.4) and (4.7), we have

$$\langle A(\vec{J})\rangle_t = \langle A(\vec{J})\rangle_{t=0} + [\langle A(\vec{J})\rangle_t]_{\delta L_1} + [\langle A(\vec{J})\rangle_t]_{\delta L_2} + [\langle A(\vec{J})\rangle_t]_{\delta L_1, \delta L_2} \tag{5.15}$$

where $[\langle A(\vec{J})\rangle_t]_{\delta L_1, \delta L_2}$ represents the interference part of (4.4) (i.e. the third summation of terms in (4.4)), $[\langle A(\vec{J})\rangle_t]_{\delta L_1}$ and $[\langle A(\vec{J})\rangle_t]_{\delta L_2}$ are the terms in

(4.4) containing either δL_1 or δL_2. Therefore, the interference part is given by

$$[\langle A(\vec{J})\rangle_t]_{\delta L_1,\delta L_2} = \langle A(\vec{J})\rangle_t - [\langle A(\vec{J})\rangle_t]_{\delta L_1} - [\langle A(\vec{J})\rangle_t]_{\delta L_1} - \langle A(\vec{J})\rangle_{t=0} \quad (5.16)$$

Numerically, we first evaluate the evolution of the expectation value under the full Hamiltonian (2.1), then subtract from it the evolution of the expectation value from the single resonance Hamiltonians (4.5) and (4.6) according to (5.16). We show the comparison between our theoretical result (the sum of λ^4, λ^6 and λ^8 contributions from Section 5.2 and 5.3) and the numerical simulation in Figure 5.3 with the same parameterization in Section 4.2.5. The dominant effect of the λ^4 contribution in the time scale of $t \sim 1/\sqrt{\lambda}$ and the appearance of oscillation with angular frequency $\omega_2/2$ is in good agreement with our theoretical predictions in Section 5.2 and 5.3.

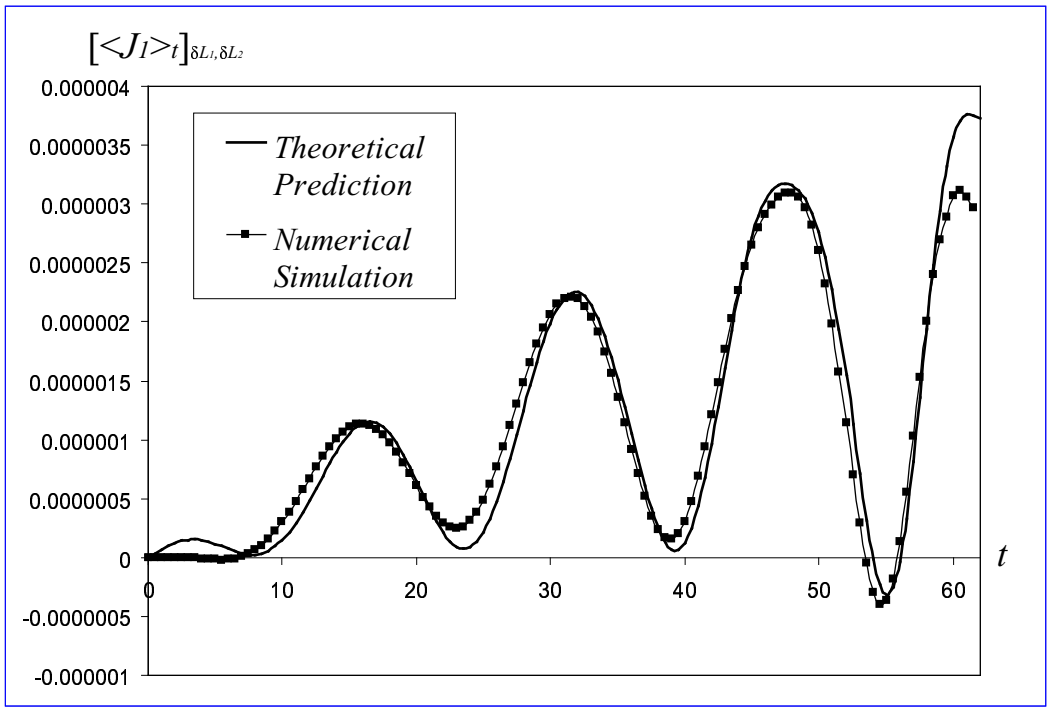

Figure 5.3: Comparison of theoretical prediction to numerical simulation for the interference part. We show the interference part of the time evolution of the expectation value $[\langle J_1 \rangle_t]_{\delta L_1, \delta L_2}$ defined in (5.16) with initial distribution function $\rho(\vec{J}, \vec{\theta}, t = 0) = (\sigma\sqrt{\pi})^{-1} \exp(-(J_1 - J_{10})^2/\sigma^2)\delta(J_2 - J_{20})$ where $\sigma = 1.0$, $J_{10} = 0.3$, and $J_{20} = 1.0$. The coupling constant is $\lambda = 0.01$ and $\omega_2 = 0.8$.

Chapter 6

Broken Time Symmetry

In this chapter, we will show that the secular effects found by evaluating the resonance effects break time symmetry.

The time reversal operator T is an anti-linear operator and defined through the following operations,

$$TJ_1 = -J_1, \qquad T\theta_1 = \theta_1 \tag{6.1}$$

for the phase space variables of the pendulum, and

$$TJ_2 = J_2, \qquad T\theta_2 = -\theta_2 \tag{6.2}$$

for the harmonic oscillator. Also, for the Fourier conjugate variables $\vec{n}$ of the angle variables, we have

$$Tn_1 = -n_1, \qquad Tn_2 = n_2 \tag{6.3}$$

The time reversal operator commutes with the Liouville operator L,

$$TL = LT \tag{6.4}$$

Hence, the operator relation with the time evolution operator $U(t) \equiv \exp(-iLt)$ is given by,

$$TU(t) = U(-t)T \tag{6.5}$$

To see the broken time symmetry, let us write the most secular effect contribution presented in (4.22) as

$$\langle A(\vec{J})\rangle_t - \langle A(\vec{J})\rangle_{t=0} \sim \int d^2J A(\vec{J})[\rho_{\vec{0}}(\vec{J},t)]_S \tag{6.6}$$

with

$$[\rho_{\vec{0}}(\vec{J},t)]_S = \Sigma(t)\rho_{\vec{0}}(\vec{J},0) \tag{6.7}$$

where the "most secular time evolution operator" $\Sigma(t)$ is defined by

$$\begin{aligned}\Sigma(t) \equiv &\left(1 + \lambda^{3/2}\pi \sum_{m=1}^{\infty} \frac{(-1)^m(\sqrt{\lambda}t)^{4m-3}a_m}{2^{2m-1}(4m-3)!}\right) \\ &\times \left(\partial_1\delta(J_1)\partial_1 + \partial_{12}\delta(J_1-\omega_2)\partial_{12}\right)\end{aligned} \tag{6.8}$$

Recall that the arguments in the delta functions $\delta(J_1)$ and $\delta(J_1-\omega_2)$ in (6.8) are the eigenvalues of the unperturbed Liouville operator L_0. Since we have $TL_0 = L_0T$, these delta functions are invariant under time reversal,

$$T\delta(\vec{n}\cdot\vec{\Omega}) = \delta(\vec{n}\cdot\vec{\Omega}) \tag{6.9}$$

Similarly, for the interaction, we have

$$T(n_1\partial_1 + n_2\partial_2) = (n_1\partial_1 + n_2\partial_2)T \tag{6.10}$$

since $T(\delta L) = (\delta L)T$ (and see (6.1) to (6.3)).

Now, applying (6.9) and (6.10) into (6.8), we obtain

$$T\Sigma(t) = \Sigma(t)T \neq \Sigma(-t)T \tag{6.11}$$

Therefore, the most secular effect breaks time symmetry.

The origin of the broken time symmetry is the resonance effect which is evaluated as the delta function. The appearance of the delta function comes from the analytic continuation of the denominator into the complex plane,

$$\frac{1}{\vec{n}\cdot\vec{\Omega}} \Rightarrow \frac{1}{\vec{n}\cdot\vec{\Omega}\pm i0} = P\frac{1}{\vec{n}\cdot\vec{\Omega}} \mp i\pi\delta(\vec{n}\cdot\vec{\Omega}) \tag{6.12}$$

where P denotes the principal part. Indeed, if (6.8) would have the off-resonance contribution from the principal part instead of the delta function part, we would have the same time symmetry as in the integrable case (6.5), since there is no factor of i in the principal part as shown in (6.12).

Note that the secular effects of the interference part discussed in Chapter 5 also come from the effect of resonance singularities in the denominators. Hence, the secular effects of the interference part also break time symmetry. Since the order of the secular effects in the interference part are different from that of the single resonance part, there is no way to compensate these secular effects and their broken time symmetry contributions.

We also note that the delta function part may contribute only under the integration over the action variables. This implies that time symmetry is broken only on the ensemble level, but not on the trajectory level.

Chapter 7

Conclusion

In this chapter, we will summarize our achievement in this thesis. We will also discuss the future direction of our research on the same subject.

We have shown that by considering the ensemble theory of small Poincaré systems, we are able to solve the small denominator problem appeared in the traditional approach of trajectory dynamics. The small denominator (propagator) is treated as a distribution (generalized function) of the resonance points under the integration over the action variables. An important aspect of this view of the denominator is that one can consistently deal with the resonance effects on the ensemble level. By applying the asymptotic perturbation analysis developed in non-equilibrium statistical mechanics, we extract the most secular effect of the expectation value of some observables which breaks time symmetry as in the case of large Poincaré systems.

However, we have found that the secular effects in the small Poincaré systems are stronger than the large Poincaré systems. The most secular effect of the single resonance part is $\lambda^{3/2}(\sqrt{\lambda}t)^{4m-3}$, $m = 1, 2, \cdots$ in contrast to the $(\lambda^2 t)^m$ secular effect in the large Poincaré systems. This distinction comes from the fact that the spectrum of the Liouville operator is continuous in the large

Poincaré systems but is discrete in the small Poincaré systems. The absence of integrations over the continuous spectrum of the Liouville operator in the small Poincaré system leads to the interference between different propagators and results in extra singularities of the resonances when we integrate over the action variables.

We have then discussed the interference between the resonances. We have shown that the most secular effect of the interference part can be evaluated in a similar way as for the single resonance case. This is important as non-integrability comes from the interference between the resonances. We are now able to evaluate quantitatively the effect of non-integrability on the level of ensemble. The secular effects of the interference part oscillate with frequencies corresponding to the higher harmonics of the system. The evaluation of the secular terms in the ensemble approach automatically takes into account the contributions from the resonance effects of these higher periodic motions. We have also shown that our approach naturally leads to the Chirikov overlapping criterion for the onset of global chaos.

In conclusion, what we have described in this thesis is a new, perturbative approach of studying analytically the secular effects of non-integrable small Poincaré systems with few degrees of freedom on the ensemble level. As shown in Chapter 6, the secular effects coming from the resonances breaks time symmetry. It should be emphasized that our treatment of the secular effects is possible only on the ensemble level but not on the trajectory level.

The future perspectives of our research on this subject are as follows:

1. So far we have only considered the case in which the observables and the initial distribution functions are independent of the angle variables. A natural extension of our calculations is to consider angle-dependent observables and initial distribution functions.

2. As mentioned in Section 5.4, it is interesting to consider the strongly-coupled case ($\omega_2 \sim \sqrt{\lambda}$) which leads to the existence of global chaos as shown in the Poincaré surface of sections in Figure 2.1c)-d). In this case, by including the less secular contributions from the interference part, one can study the effect of higher order resonances on the chaotic behavior from the statistical point of view. More importantly, this consideration allows us to discuss the relations between the higher order resonance effects and irreversibility in chaotic systems on the level of ensemble.

3. The time dependent perturbation analysis discussed in this thesis is an initial value problem of the time evolution of the system. As mentioned in Introduction, the asymptotic perturbation analysis in the time dependent approach is a starting point of modern kinetic theory based on the time independent analysis, such as the extension of the unitary (or canonical) transformation for the non-integrable large Poincaré systems. It is quite interesting to extend our approach to the similar level of time independent analysis for the small Poincaré systems.

Appendices

Appendix A

Poincaré's Theorem

In this appendix, we will discuss the Poincaré's theorem on the non-existence of uniform invariants for certain class of Hamiltonian systems. We will follow very closely the method due to Poincaré [16, 17].

The Poincaré's theorem concerns Hamiltonian systems with N degrees of freedom

$$\begin{aligned} H(\vec{J},\vec{\theta}) &= H_0(\vec{J}) + \lambda V(\vec{J},\vec{\theta}) \\ V(\vec{J},\vec{\theta}) &= \sum_{\vec{n}} V_{\vec{n}}(\vec{J}) e^{i\vec{n}\cdot\vec{\theta}} \end{aligned} \tag{A.1}$$

where $\vec{J} = \{J_1, \cdots, J_N\}$ and $\vec{\theta} = \{\theta_1, \cdots, \theta_N\}$ are the action-angle variables, $\vec{n} = \{n_1, \cdots, n_N\}$ are the Fourier conjugate variables of the angle variables. We assume that the Hessian of the unperturbed Hamiltonian does not vanish, i.e.

$$\det \left| \frac{\partial^2 H_0}{\partial J_i \partial J_j} \right| \neq 0 \qquad i,j = 1, 2, \cdots, N \tag{A.2}$$

The Poincaré's theorem asserts that if this system satisfies the condition of dissipativity[1], namely the Fourier coefficient of the potential energy $V_{\vec{n}}(\vec{J})$

[1] Here, we have followed Prigogine's terminology in non-equilibrium statistical mechanics of large Poincaré systems [17].

does not vanish when the resonance conditions

$$\vec{n} \cdot \vec{\Omega}(\vec{J}) = 0 \quad \text{with} \quad \vec{\Omega}(\vec{J}) = \frac{\partial H_0(\vec{J})}{\partial \vec{J}} \tag{A.3}$$

are satisfied, there is no uniform invariant of motion $\Phi(\vec{J}, \vec{\theta}, \lambda)$ which is single-valued and regular in $\vec{J}$, $\vec{\theta}$ and λ other than the Hamiltonian (and the function of it). In other words, the Hamiltonian (A.1) is non-integrable if the condition of dissipativity is satisfied. The proof of the theorem is sketched as follows.

We consider an invariant of motion Φ which is analytic in the coupling constant λ so that it can be expanded in a Taylor series in λ

$$\Phi(\vec{J}, \vec{\theta}, \lambda) = \sum_{r=0}^{\infty} \lambda^r \Phi^{(r)}(\vec{J}, \vec{\theta}) \tag{A.4}$$

Moreover, since Φ is periodic in the angle variables, we can expand each $\Phi^{(r)}$ in a Fourier series

$$\Phi^{(r)}(\vec{J}, \vec{\theta}) = \sum_{\vec{n}} \varphi_{\vec{n}}^{(r)}(\vec{J}) e^{i\vec{n}\cdot\vec{\theta}} \tag{A.5}$$

The basic question is then whether it is possible to find the invariant Φ which reduces to Φ_0 when $\lambda \to 0$. Φ is an invariant of motion implies

$$L\Phi = i\{H, \Phi\} = 0 \tag{A.6}$$

where L is the Liouville operator and $\{\cdot, \cdot\}$ is the Poisson bracket. From (A.1), (A.4) and equating power of λ, we have

$$\begin{aligned} &\{H_0, \Phi^{(0)}\} = 0 \\ &\{H_0, \Phi^{(r)}\} + \{V, \Phi^{(r-1)}\} = 0 \qquad r = 1, 2, \cdots \end{aligned} \tag{A.7}$$

We first show that the leading term $\Phi^{(0)}$ can be chosen to be independent of H_0. Suppose $\Phi^{(0)} = f(H_0)$ is a function of H_0, one can then form the invariant $\Phi - f(H)$. For $\lambda \to 0$, this invariant vanishes, we may then write

$$\begin{aligned} \Phi - f(H) &= \lambda(\Phi'^{(0)} + \lambda\Phi'^{(1)} + \cdots) \\ &= \lambda\Phi' \end{aligned} \tag{A.8}$$

where Φ' is again an invariant. Now either $\Phi'^{(0)}$ is no longer a function of H_0 or we may repeat the operation. Therefore, if $\Phi^{(0)}$ is a function of H_0, we may always find another invariant whose leading term is not a function of H_0 except in the trivial case in which Φ is a function of H.

Next, we show that $\Phi^{(0)}$ is a function of the actions only. Indeed, using (A.5) and the first equation of (A.7), we have

$$(\vec{n} \cdot \vec{\Omega}(\vec{J}))\varphi^{(0)}_{\vec{n}}(\vec{J}) = 0 \tag{A.9}$$

This implies $\varphi^{(0)}_{\vec{n}} = 0$ or $\vec{n} \cdot \vec{\Omega} = 0$. But the second condition can only be satisfied identically for all value of $\vec{J}$ if $\vec{n} = 0$. Therefore we conclude that

$$\varphi^{(0)}_{\vec{n}}(\vec{J}) = 0 \quad \text{except for} \quad \vec{n} = 0 \tag{A.10}$$

We now consider the first order contribution ($r = 1$) of (A.7). By using the Fourier expansion (A.5) and the fact that $\Phi^{(0)}$ is independent of the angle variables, we have

$$(\vec{n} \cdot \vec{\Omega}(\vec{J}))\varphi^{(1)}_{\vec{n}}(\vec{J}) = \left(\vec{n} \cdot \frac{\partial \Phi^{(0)}(\vec{J})}{\partial \vec{J}}\right) V_{\vec{n}}(\vec{J}) \tag{A.11}$$

where $V_{\vec{n}}$ is the Fourier coefficient of the interaction defined in (A.1). Thus, if the condition of dissipativity is satisfied, we have at every point where the resonance condition (A.3) is satisfied

$$\vec{n} \cdot \frac{\partial \Phi^{(0)}(\vec{J})}{\partial \vec{J}} = 0 \tag{A.12}$$

This equation is therefore a consequence of the validity of the resonance condition (A.3) and for all points for which (A.3) is satisfied, we have

$$\frac{\Omega_1(\vec{J})}{(\partial \Phi^{(0)}(\vec{J})/\partial J_1)} = \frac{\Omega_2(\vec{J})}{(\partial \Phi^{(0)}(\vec{J})/\partial J_2)} = \cdots = \frac{\Omega_N(\vec{J})}{(\partial \Phi^{(0)}(\vec{J}))/\partial J_N)} \tag{A.13}$$

The crucial point in Poincaré's proof is to show that the resonance condition have so "many" solutions and (A.13) has to be valid identically.

To demonstrate this point, We consider the system (2.1) and (2.2) discussed in this thesis. The Hessian

$$\begin{vmatrix} \frac{\partial^2 H_0(\vec{J})}{\partial J_1^2} & \frac{\partial^2 H_0(\vec{J})}{\partial J_1 \partial J_2} \\ \frac{\partial^2 H_0(\vec{J})}{\partial J_2 \partial J_1} & \frac{\partial^2 H_0(\vec{J})}{\partial^2 J_2} \end{vmatrix} = \begin{vmatrix} 1 & 0 \\ 0 & 0 \end{vmatrix} = 0 \tag{A.14}$$

vanishes and this circumstance would prove inconvenient in the proof of the Poincaré's theorem, we will modify the form of the Hamiltonian so that the corresponding Hessian is not zero.

Let us write $K = H^2$ where $H = H(\vec{J}, \vec{\theta})$ in (2.1). Also let $H = E$ be the integral of energy. Then the equation of motion of our system (2.3) can be written in the form

$$\begin{aligned} \frac{d\vec{J}}{dt} &= -\frac{1}{2E}\frac{\partial K(\vec{J}, \vec{\theta})}{\partial \vec{\theta}} \\ \frac{d\vec{\theta}}{dt} &= \frac{1}{2E}\frac{\partial K(\vec{J}, \vec{\theta})}{\partial \vec{J}} \end{aligned} \tag{A.15}$$

Therefore, if we restrict ourselves on the energy surface with energy E, we can take a new function $H = K/2E$ and write the equation of motion in the canonical form

$$\begin{aligned} \frac{d\vec{J}}{dt} &= -\frac{\partial H(\vec{J},\vec{\theta})}{\partial \vec{\theta}} \\ \frac{d\vec{\theta}}{dt} &= \frac{\partial H(\vec{J},\vec{\theta})}{\partial \vec{J}} \end{aligned} \tag{A.16}$$

where H_0 now have the form

$$2EH_0(\vec{J},\vec{\theta}) = (\frac{J_1^2}{2} + \omega_2 J_2)^2 = \frac{J_1^4}{4} + \omega_2 J_1^2 J_2 + \omega_2^2 J_2^2 \tag{A.17}$$

The Hessian of H_0 in (A.17) is now not zero. With this form of H_0, the resonance condition (A.3) then becomes

$$n_1\Omega_1(\vec{J}) + n_2\Omega_2(\vec{J}) = n_1(J_1^3 + 2\omega_2 J_1 J_2) + n_2(\omega_2 J_1^2 + 2\omega_2^2 J_2) = 0 \tag{A.18}$$

This means that the frequencies Ω_1 and Ω_2 are commensurable with each other. Therefore, in each domain of variation of Ω_1 and Ω_2, there are an infinite number of values of Ω_1 and Ω_2 for which the resonance condition (A.3) is satisfied. Since the Hessian is not zero, this also implies that there are an infinite number of values of the action variables J_1 and J_2 satisfy the resonance condition (A.3).

As a result, if we restrict ourselves to $\Phi^{(0)}$'s that are continuous functions, the relation (A.13) must be satisfied identically. This means that all determinants

$$\begin{vmatrix} J_i & J_j \\ \partial\Phi^0/\partial J_i & \partial\Phi^0/\partial J_j \end{vmatrix} \tag{A.19}$$

vanish with $i, j = 1, 2, \cdots, N$. Equation (A.19) is precisely the condition that $\Phi^{(0)}$ be a function of H_0, i.e.

$$F(\Phi^{(0)}, H_0) = 0 \tag{A.20}$$

To see this, we differentiate (A.20) with respect to J_i and J_j respectively, it follows that

$$\begin{aligned} \frac{\partial F}{\partial \Phi^{(0)}} \frac{\partial \Phi^{(0)}}{\partial J_i} + \frac{\partial F}{\partial H_0} \Omega_i = 0 \\ \frac{\partial F}{\partial \Phi^{(0)}} \frac{\partial \Phi^{(0)}}{\partial J_j} + \frac{\partial F}{\partial H_0} \Omega_j = 0 \end{aligned} \tag{A.21}$$

These relations are just equivalent to (A.19).

We have therefore shown that $\Phi^{(0)}$ has to be a function of H_0 in contradiction to our previous result that we may restrict ourselves to invariants which are not functions of H_0. This implies that there is no uniform invariant of motion except for the Hamiltonian for systems satisfying the condition of dissipativity.

Appendix B

Overview of $\lambda^2 t$-Approximation for the Large Poincaré System

In this appendix, we will summarize the derivation of the $\lambda^2 t$-approximation for the large Poincaré system by considering the weakly coupled gas system. This discussion has no mean to give a complete survey in the subject but a brief review on the essential ingredients in the derivation of the $\lambda^2 t$-approximation. A more completed review of the subject can be found in [1, 7, 8, 17].

We start with the Hamiltonian of N weakly interacting particles

$$H(p,q) = \sum_i \frac{p_i^2}{2m} + \lambda \sum_{j>n} V_{jn}(|\vec{q}_j - \vec{q}_n|) \tag{B.1}$$

where $\lambda \ll 1$ is the coupling constant, $q = \{\vec{q}_1, \cdots, \vec{q}_N\}$ and $p = \{\vec{p}_1, \cdots, \vec{p}_N\}$ are the N-component position and momentum vectors. The system is put into a large box of volume L^3 with periodic boundary condition. It is well known that this system is in general non-integrable in the sense of Poincaré (see Appendix A). The "thermodynamic limit" of the system corresponds to

$$N \to \infty, \quad \text{and} \quad L^3 \to \infty \quad \text{with} \quad c = N/L^3 = \text{finite}. \tag{B.2}$$

As usual, the interaction potential V_{jn} and the distribution function

$\rho(p,q,t)$ are expanded in Fourier series

$$\begin{aligned} V_{jn}(|\vec{q}_j - \vec{q}_n|) &= \frac{8\pi^3}{L^3} \sum_{\vec{l}} V_{\vec{l}}\, e^{i\vec{l}\cdot(\vec{q}_j - \vec{q}_n)} \\ \rho(p,q,t) &= \frac{1}{L^{3N}} \sum_{\{\vec{k}\}} \rho_{\{\vec{k}\}}(p,t) e^{i\sum_j \vec{k}_j \cdot \vec{q}_j} \end{aligned} \tag{B.3}$$

where $\vec{l} = 2\pi\vec{n}/L$ and $\vec{n} = \{n_1, n_2, n_3\}$ are integers. The Liouville operator is given by

$$\begin{aligned} L &= L_0 + \lambda \delta L \\ L_0 &= -i \sum_j \frac{\vec{p}_j}{m} \cdot \frac{\partial}{\partial \vec{q}_j} \\ \delta L &= i \sum_{j>n} \frac{\partial V_{jn}}{\partial \vec{q}_j} \cdot \left[\frac{\partial}{\partial \vec{p}_j} - \frac{\partial}{\partial \vec{p}_n} \right] \\ &= -\frac{8\pi^3}{L^3} \sum_{j<n} \sum_{\vec{l}} V_{\vec{l}}\, e^{i\vec{l}\cdot(\vec{q}_j - \vec{q}_n)}\, \vec{l} \cdot \left[\frac{\partial}{\partial \vec{p}_j} - \frac{\partial}{\partial \vec{p}_n} \right] \end{aligned} \tag{B.4}$$

The eigenfunctions of the unperturbed Liouville operator can be solved to be

$$\Phi_{\{\vec{k}\}}(\vec{q}) = \langle \vec{q} | \{\vec{k}\} \rangle = \frac{1}{L^{3N/2}} e^{i\sum_j \vec{k}_j \cdot \vec{q}_j} \tag{B.5}$$

with eigenvalues

$$L_0 | \{\vec{k}\} \rangle = \left[\sum_j \frac{\vec{p}_j}{m} \cdot \vec{k}_j \right] | \{\vec{k}\} \rangle \tag{B.6}$$

where the brac-ket notation has been used. The matrix element of the per-

turbed Liouville operator is defined as

$$\begin{aligned}
&\langle\{\vec{k}\}|\delta L|\{\vec{k}'\}\rangle \\
&\quad = \frac{1}{L^{3N}}\int d^3q_1\cdots d^3q_N e^{-i\sum_j \vec{k}_j\cdot\vec{q}_j}\delta L e^{i\sum_j \vec{k}'_j\cdot\vec{q}_j} \\
&\quad = -\left(\frac{8\pi^3}{L^3}\right)\left(\frac{1}{L^{3N}}\right)\sum_{j<n}\sum_{\vec{l}}\int d^3q_1\cdots d^3q_N e^{-i\sum_r \vec{k}_r\cdot\vec{q}_r} e^{i\vec{l}\cdot(\vec{q}_j-\vec{q}_n)} \\
&\qquad \times V_{\vec{l}}\,\vec{l}\cdot\left(\frac{\partial}{\partial\vec{p}_j}-\frac{\partial}{\partial\vec{p}_n}\right)e^{i\sum_r \vec{k}'_r\cdot\vec{q}_r}
\end{aligned} \tag{B.7}$$

After performing the integrations $\int d^3q_1\cdots d^3q_N$ by using the identity

$$\int d^3q e^{-i\vec{k}\cdot\vec{q}} = L^3\delta^{\mathrm{Kr}}_{\vec{k}} \tag{B.8}$$

where $\delta^{\mathrm{Kr}}_{\vec{k}}$ is the Kronecker delta function, i.e. $\delta^{\mathrm{Kr}}_{\vec{k}}=1$ if $\vec{k}=0$ and $\delta^{\mathrm{Kr}}_{\vec{k}}=0$ if $\vec{k}\neq 0$, the only non-zero matrix elements can be found in the form

$$\begin{aligned}
\delta L_{jn}(\vec{l}) &= \langle\{\vec{k}\}|\delta L|\vec{k}_j-\vec{l},\vec{k}_n+\vec{l},\{\vec{k}'\}\rangle \\
&= -\frac{8\pi^3}{L^3}V_{\vec{l}}\,\vec{l}\cdot\left[\frac{\partial}{\partial\vec{p}_j}-\frac{\partial}{\partial\vec{p}_n}\right]
\end{aligned} \tag{B.9}$$

Because the interaction we considered is binary, the set $\{\vec{k}'\}$ equals to $\{\vec{k}\}$ in (B.9) except for the j-th and n-th particles.

It is now ready to perform the time dependent perturbation analysis by using the resolvent formalism discussed in Section 3.2. For simplicity, we will consider the evolution of the zeroth Fourier mode of the distribution function (i.e. $\rho_{\{\vec{0}\}}(p,t)$) with initial condition $\rho(p,q,t=0)=\rho_{\{\vec{0}\}}(p,t=0)/L^{3N}$ as in the previous chapters. Following (3.15) and (3.19), we express the evolution

of $\rho_{\{\vec{0}\}}(p,t)$ in terms of the resolvent

$$\begin{aligned}\rho_{\{\vec{0}\}}(p,t) = \frac{-1}{2\pi i}\int_C dz e^{-izt}\sum_{m=0}^{\infty}(-\lambda)^m\langle\{\vec{0}\}|\frac{1}{L_0-z} \\ \times\left(\delta L\frac{1}{L_0-z}\right)^m|\{\vec{0}\}\rangle\rho_{\{\vec{0}\}}(p,t=0)\end{aligned} \tag{B.10}$$

Now let us review the procedure in extracting the most secular terms from this expression in the thermodynamic limit order by order.

B.1 Zeroth and First order

The zeroth order is the unperturbed motion

$$\rho^{(0)}_{\{\vec{0}\}} = \frac{1}{2\pi i}\int_C dz\frac{e^{-izt}}{z}\rho_{\{\vec{0}\}}(p,t=0) = \rho_{\{\vec{0}\}}(p,t=0) \tag{B.11}$$

where the superscript (0) indicates the order of approximation. The first order contribution, and in fact all the odd order contributions, vanishes since there is no transition from $|\{\vec{0}\}\rangle$ to $|\{\vec{0}\}\rangle$ in odd number of steps.

B.2 Second order

From (B.10), the second order term is

$$\rho^{(2)}_{\{\vec{0}\}}(p,t) = \frac{-\lambda^2}{2\pi i}\int_C dz\frac{e^{-izt}}{z^2}\Phi(z)\rho_{\{\vec{0}\}}(p,t=0) \tag{B.12}$$

where

$$\begin{aligned}\Phi(z) &\equiv \langle\{\vec{0}\}|\delta L\frac{1}{L_0-z}\delta L|\{\vec{0}\}\rangle \\ &= \left(\frac{8\pi^3}{L^3}\right)^2\sum_{\vec{l}}\sum_{j>n}\vec{l}\cdot\left[\frac{\partial}{\partial\vec{p}_j}-\frac{\partial}{\partial\vec{p}_n}\right]\frac{|V_{\vec{l}}|^2}{\vec{l}\cdot(\vec{p}_n-\vec{p}_j)/m-z}\,\vec{l}\cdot\left[\frac{\partial}{\partial\vec{p}_j}-\frac{\partial}{\partial\vec{p}_n}\right]\end{aligned} \tag{B.13}$$

is the well-known collision operator. Within the summation over $\vec{l}$ in the collision operator, each component of $\vec{l} = \{l_1, l_2, l_3\}$ runs from $-\infty$ to $+\infty$ excluding $\vec{l} = 0$. By changing the negative arguments in l_1 by $-l_1$, the collision operator becomes

$$\Phi(z = i0^+) = \left(\frac{8\pi^3}{L^3}\right)^2 \sum_{\vec{l},\, l_1>0} \sum_{j>n} \vec{l}\cdot\left[\frac{\partial}{\partial\vec{p}_j} - \frac{\partial}{\partial\vec{p}_n}\right] |V_{\vec{l}}|^2 \left[\frac{1}{\vec{l}\cdot(\vec{p}_n - \vec{p}_j)/m - i0^+}\right.$$
$$\left. - \frac{1}{\vec{l}\cdot(\vec{p}_n - \vec{p}_j)/m + i0^+}\right] \vec{l}\cdot\left[\frac{\partial}{\partial\vec{p}_j} - \frac{\partial}{\partial\vec{p}_n}\right] \tag{B.14}$$

Since it is well known that the most secular effect is obtained by taking the asymptotic limit $z \to i0^+$, we have replaced z by $i0^+$ in the above equation. In the thermodynamic limit, $L \to \infty$, the eigenspectrum of the unperturbed Liouville operator becomes continuous $\Delta l = 2\pi/L \to 0$ so that the summation over $\vec{l}$ in the collision operator can be replaced by the integration, i.e.

$$\frac{8\pi^3}{L^3} \sum_{\vec{l}} \to \int d^3l \tag{B.15}$$

Moreover, by using the identity

$$\frac{1}{x - i0^+} - \frac{1}{x + i0^+} = 2\pi i\delta(x) \tag{B.16}$$

where $\delta(x)$ is the Dirac delta function, the collision operator becomes

$$\Phi(i0^+) = \frac{8\pi^3}{L^3} \sum_{j>n} \int_{l_1>0} d^3l\ \vec{l}\cdot\left[\frac{\partial}{\partial\vec{p}_j} - \frac{\partial}{\partial\vec{p}_n}\right] |V_{\vec{l}}|^2 \delta(\vec{l}\cdot(\vec{p}_n - \vec{p}_j)/m)\ \vec{l}\cdot\left[\frac{\partial}{\partial\vec{p}_j} - \frac{\partial}{\partial\vec{p}_n}\right] \tag{B.17}$$

in the thermodynamic limit. Therefore, we see that the collision operator does not vanish if the resonance condition $\vec{l}\cdot(\vec{p}_n - \vec{p}_j)/m = 0$ is satisfied due to the

delta function. As a result, the most secular time dependence of (B.12) is

$$\rho^{(2)}_{\{\vec{0}\}}(p,t) \sim \lambda^2 \Phi(i0^+) \int_C dz \frac{e^{-izt}}{z^2} \rho_{\vec{0}}(p, t=0) \sim \lambda^2 t \tag{B.18}$$

where $\sim$ means only the most secular effect has been kept.

We note that the above calculation makes sense only in the thermodynamic limit so that the delta function can be integrated under the continuous wave vector integration. However, in the case of small Poincaré system, the eigenspectrum of the unperturbed Liouville operator is discrete so that an integration over the wave vector is absence. As discussed in the text, it is therefore necessary to consider the time evolution of expectation values instead of the distribution function for small Poincaré system. In such way, the integration of the delta function can still be performed by integrating over the continuous action variables.

B.3 Higher Order

The transition in (B.12) and (B.13) that gives the most secular effect in the second order calculation is called "diagonal fragment". One can show that in the case of general even order λ^{2m}, the most secular effect is given by

a succession of n diagonal fragments [17], i.e.

$$\begin{aligned}\rho_{\vec{0}}^{(2m)}(p,t) \sim & -\frac{\lambda^{2m}}{2\pi i}\int_C dz e^{-izt}\left(\frac{1}{-z}\right)\langle\{\vec{0}\}|\delta L\frac{1}{L_0-z}\delta L|\{\vec{0}\}\rangle\left(\frac{1}{-z}\right)\\ & \times\cdots\left(\frac{1}{-z}\right)\langle\{\vec{0}\}|\delta L\frac{1}{L_0-z}\delta L|\{\vec{0}\}\rangle\left(\frac{1}{-z}\right)\rho_{\vec{0}}(p,t=0)\\ \sim & -\frac{\lambda^{2m}}{2\pi i}\int_C dz e^{-izt}\left(\frac{1}{-z}\right)\Phi(z)\left(\frac{1}{-z}\right)\Phi(z)\\ & \times\cdots\Phi(z)\left(\frac{1}{-z}\right)\Phi(z)\left(\frac{1}{-z}\right)\rho_{\vec{0}}(p,t=0)\end{aligned} \tag{B.19}$$

and there are m collision operators in (B.19). Thanks to the integration over the continuous wave vector, the collision operator $\Phi(i0^+)$ is well-defined as in the second order term calculation (see (B.17)). Therefore the most secular effect of (B.19) can be found easily as

$$\begin{aligned}\rho_{\vec{0}}^{(2m)}(p,t) &\sim -\frac{\lambda^{2m}}{2\pi i}[\Phi(i0^+)]^m\int_C dz e^{-izt}\left(\frac{1}{-z}\right)^{m+1}\rho_{\vec{0}}(p,t=0)\\ &\sim \lambda^{2m}t^m\end{aligned} \tag{B.20}$$

(B.20) then gives the λ^{2m}-order most secular effect of the $\lambda^2 t$-approximation of the large Poincaré system.

However, since the eigenspectrum of the unperturbed Liouville operator is discrete for small Poincaré system, there is no integration over the wave vector as in (B.17) for the collision operator. In this case, the collision operator would in general be a distribution (generalized function) and the appearance of product of distributions leads to a stronger secular effect for small Poincaré system (see Chapter 4 and 5).

Appendix C

Diagrammatic Representation

We will discuss the Prigogine and Henin's diagrammatic representation for a general transition (3.20) of order λ^k (k even) in this appendix. The expression for such transition with intermediate states $|\vec{0}\rangle \leftarrow |\vec{n}^{(k-1)}\rangle \leftarrow \cdots \leftarrow |\vec{n}^{(1)}\rangle \leftarrow |\vec{0}\rangle$ reads

$$\begin{aligned}
&\frac{-\lambda^k}{2\pi i}\int d^2J A(\vec{J})\int_C dz e^{-izt}\left(\frac{1}{-z}\right)\langle\vec{0}|\delta L|\vec{n}^{(k-1)}\rangle\frac{1}{\vec{n}^{(k-1)}\cdot\vec{\Omega}-z} \\
&\quad\times\langle\vec{n}^{(k-1)}|\delta L|\vec{n}^{(k-2)}\rangle\frac{1}{\vec{n}^{(k-2)}\cdot\vec{\Omega}-z}\cdots\langle\vec{n}^{(2)}|\delta L|\vec{n}^{(1)}\rangle\frac{1}{\vec{n}^{(1)}\cdot\vec{\Omega}-z} \\
&\quad\times\langle\vec{n}^{(1)}|\delta L|\vec{0}\rangle\left(\frac{1}{-z}\right)\rho_{\vec{0}}(\vec{J},0)
\end{aligned} \tag{C.1}$$

where $\vec{\Omega}=\{J_1,\omega_2\}$. In order to represent (C.1) using diagrams, we first note that only the wave numbers $\{n_1^{(i)},n_2^{(i)}\}$ labeling the intermediate states are explicitly modified by the interactions, so we represent only these numbers graphically. But it should keep in mind that the action variables $\vec{J}$ are also affected by the interaction through the differential operators $\partial/\partial\vec{J}$.

In general, an intermediate state $|n_1,n_2\rangle$ is represented by n_1 (with label "1") and n_2 (with label "2") directed lines; lines directed from right to left corresponds to positive value of $n_{1,2}$ while negative values of $n_{1,2}$ are represented by lines directed from left to right. For example, Figure C.1a) shows

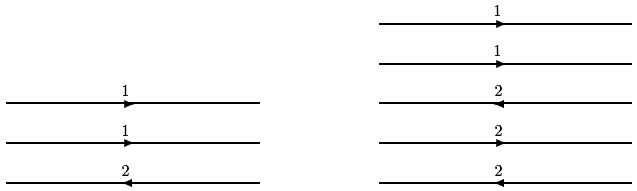

Figure C.1: Diagrammatic representation of the state $|-2,1\rangle$

the state $|n_1 = -2, n_2 = 1\rangle$. We also adopt the convention that lines having the same label can be added algebraically. Therefore the state represented by Figure C.1a) may also be represented by Figure C.1b).

Note that the interaction modifies the state of the system so that a transition $\langle\vec{n}|\delta L|\vec{n}'\rangle$ brings the system from the state $|\vec{n}'\rangle$ to the state $|\vec{n}\rangle$. We represent each transition by a vertex with directed lines attached to it. Recall from (4.2) and (4.3) that the allowable transitions for the system considered in this thesis are $\langle n_1, n_2|\delta L|n_1 \pm 1, n_2\rangle$ for the resonance at $J_1 = 0$ and $\langle n_1, n_2|\delta L|n_1 \pm 1, n_2 \mp 1\rangle$ for the resonance at $J_1 = \omega_2$. The corresponding vertices for these transitions are shown in Figure C.2 together with their mathematical expressions according to (4.2) and (4.3).

Thus given a general transition (C.1) of order λ^k, one reads the expression from right to left, starting with no lines since the initial state is $|\vec{0}\rangle$, then each of the interaction which leads the system to the intermediate states $|\vec{n}^{(1)}\rangle$, $|\vec{n}^{(2)}\rangle$,$\cdots$ are represented by the corresponding vertex in Figure C.2 and the number of vertices in the diagram equals to the order of the transition

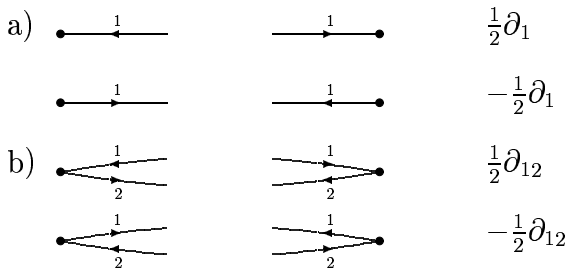

Figure C.2: Allowable vertices and their mathematical expression. Vertices in a) correspond to the transitions $\langle n_1, n_2|\delta L_1|n_1 \pm 1, n_2\rangle$ for the resonance at $J_1 = 0$, vertices in b) correspond to the transitions $\langle n_1, n_2|\delta L_2|n_1 \pm 1, n_2 \mp 1\rangle$ for the resonance at $J_1 = \omega_2$. The right column gives the mathematical expression of the vertices.

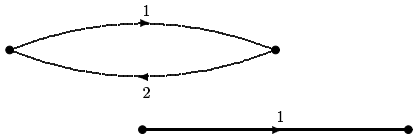

Figure C.3: The diagrammatic representation of (C.2)

considered. For example, the expression

$$\begin{aligned}
&\frac{-\lambda^4}{2\pi i}\int d^2JA(\vec{J})\int_C dz e^{-izt}\left(\frac{1}{-z}\right)\langle\vec{0}|\delta L|-1,1\rangle\frac{1}{-J_1+\omega_2-z}\\
&\quad\times\langle -1,1|\delta L|-2,1\rangle\frac{1}{-2J_1+\omega_2-z}\langle -2,1|\delta L|-1,0\rangle\frac{1}{-J_1-z} \qquad \text{(C.2)}\\
&\quad\times\langle -1,0|\delta L|\vec{0}\rangle\left(\frac{1}{-z}\right)\rho_{\vec{0}}(\vec{J},0)
\end{aligned}$$

is represented by Figure C.3.

Inversely, for a given diagram, the corresponding expression can be generated by applying the following rules:

1. Associate to each intermediate state (include initial and final) the corresponding propagator $(\vec{n} \cdot \vec{\Omega} - z)^{-1}$ with $\vec{\Omega} = \{J_1, \omega_2\}$.

2. Associate to each vertex (interaction) the corresponding matrix element $\langle \vec{n} | \delta L | \vec{n}' \rangle$. These matrix elements and propagators must be arranged in the same order as the lines and vertices in the diagram.

3. Then, multiple from the right the initial distribution $\rho_{\vec{0}}(\vec{J}, t = 0)$.

4. Finally, multiply on the left by the expression

   $-\lambda^k/(2\pi i) \int d^2J A(\vec{J}) \int_C dz \exp(-izt)$

   with k the number of vertices in the diagram studied.

Appendix D

Proof of Equation (4.22) and (4.23)

We will derive the general expression in (4.22) and (4.23) in this appendix. According to (3.20) and Appendix C, the mathematical expression of a transition of order λ^{2m} with intermediate states $|\vec{0}\rangle \leftarrow |\vec{n}^{(2m-1)}\rangle \leftarrow \cdots \leftarrow |\vec{n}^{(1)}\rangle \leftarrow |\vec{0}\rangle$ is given by

$$\begin{aligned}
&\frac{-\lambda^{2m}}{2\pi i}\int d^2JA(\vec{J})\int_C dz e^{-izt}\left(\frac{1}{-z}\right)\langle\vec{0}|\delta L|\vec{n}^{(2m-1)}\rangle\frac{1}{\vec{n}^{(2m-1)}\cdot\vec{\Omega}-z}\\
&\times\langle\vec{n}^{(2m-1)}|\delta L|\vec{n}^{(2m-2)}\rangle\frac{1}{\vec{n}^{(2m-2)}\cdot\vec{\Omega}-z}\cdots\langle\vec{n}^{(2)}|\delta L|\vec{n}^{(1)}\rangle \qquad \text{(D.1)}\\
&\times\frac{1}{\vec{n}^{(1)}\cdot\vec{\Omega}-z}\langle\vec{n}^{(1)}|\delta L|\vec{0}\rangle\left(\frac{1}{-z}\right)\rho_{\vec{0}}(\vec{J},0)
\end{aligned}$$

where $\vec{\Omega}=\{J_1,\omega_2\}$ and the allowable transitions $\langle\vec{n}^{(i)}|\delta L|\vec{n}^{(i-1)}\rangle$ given in (4.2) and (4.3) can take the form

$$\langle\vec{n}^{(i)}|\delta L|\vec{n}^{(i-1)}\rangle=\pm\frac{1}{2}(\partial_1-\sigma^{(i)}\partial_2),\ \sigma^{(i)}=\begin{cases}0 & \text{for the resonance } J_1=0,\\ 1 & \text{for the resonance } J_1=\omega_2.\end{cases} \qquad \text{(D.2)}$$

where $\partial_{1,2}=\partial/\partial J_{1,2}$ and $\partial_{12}=\partial_1-\partial_2$. By following the same procedure in Section 4.2.2, we evaluate the most secular effect of (D.1) by calculating the

residues, i.e.

$$(-1)^m(2\pi i)\left(\frac{\lambda}{2}\right)^{2m}\operatorname*{Res}_{z=i0}\operatorname*{Res}_{J_1=\{\xi\}}\left[\frac{e^{-izt}}{z^2}\int dJ_2((\partial_1-\sigma^{(2m)}\partial_2)A(\vec{J}))\right.$$
$$\times\left\{\frac{1}{\vec{n}^{(2m-1)}\cdot\vec{\Omega}-z}(\partial_1-\sigma^{(2m-1)}\partial_2)\frac{1}{\vec{n}^{(2m-2)}\cdot\vec{\Omega}-z}\cdots(\partial_1-\sigma^{(2)}\partial_2)\frac{1}{\vec{n}^{(1)}\cdot\vec{\Omega}-z}\right\}$$
$$\left.\times(\partial_1-\sigma^{(1)}\partial_2)\rho_{\vec{0}}(\vec{J},0)\right] \tag{D.3}$$

where $\{\xi\}$ is the set of poles of the expression inside the curly bracket on the upper half complex-J_1 plane. In (D.3), the residue in J_1 should be evaluated before taking the residue at $z=0$. It should also be understood that the derivative operators ∂_1 and ∂_2 inside the curly bracket of (D.3) act on everything to the right.

Note that extracting the most secular effect (i.e. the highest power in t) from (D.3) means extracting the highest order pole at $z=0$. We proceed by observing that the following operations do not change the highest order pole structure of (D.3).

1. The highest order pole in z is obtained if the derivative operators ∂_1 inside the curly bracket act on the propagators $1/(\vec{n}^{(i)}\cdot\vec{\Omega}-z)$ with $i=1,2,\cdots,2m-1$, so we can bring the factor $(\partial_1-\sigma^{(1)}\partial_2)\rho_{\vec{0}}(\vec{J},0)$ to the front of the curly bracket without changing the highest order pole in z.

2. The derivative operators ∂_2 inside the curly bracket do not change the most secular effect and can be dropped. This is because all the propagators $1/(\vec{n}^{(i)}\cdot\vec{\Omega}-z)$ depend only on J_1 for our system.

After these operations, we have

$$
\begin{aligned}
&(-1)^m(2\pi i)\left(\frac{\lambda}{2}\right)^{2m} \\
&\times \operatorname*{Res}_{z=i0}\operatorname*{Res}_{J_1=\{\xi\}}\left[\int dJ_2((\partial_1-\sigma^{(2m)}\partial_2)A(\vec{J}))((\partial_1-\sigma^{(1)}\partial_2)\rho_{\vec{0}}(\vec{J},0))\right|_{J_1=\xi_i} \\
&\times\left\{\frac{e^{-izt}}{z^2}\frac{1}{\vec{n}^{(2m-1)}\cdot\vec{\Omega}-z}\partial_1\frac{1}{\vec{n}^{(2m-2)}\cdot\vec{\Omega}-z}\cdots\partial_1\frac{1}{\vec{n}^{(1)}\cdot\vec{\Omega}-z}\right\}\Bigg]
\end{aligned}
\tag{D.4}
$$

Therefore, the leading pole of z in (D.4) is then determined by the expression

$$
\begin{aligned}
&\frac{1}{z^2}\operatorname*{Res}_{J_1=\{\xi_i\}}\left[\frac{1}{\vec{n}^{(2m-1)}\cdot\vec{\Omega}-z}\partial_1\frac{1}{\vec{n}^{(2m-2)}\cdot\vec{\Omega}-z}\partial_1\cdots\partial_1\frac{1}{\vec{n}^{(1)}\cdot\vec{\Omega}-z}\right] \\
&\sim\frac{1}{z^{4m-2}}
\end{aligned}
\tag{D.5}
$$

(4.23) is then obtained by summing over all most secular transitions of order λ^{2m}.

Bibliography

[1] R. Balescu. *Statistical mechanics of charged particles.* Monographs in statistical physics and thermodynamics. Interscience, 1963.

[2] R. Balescu. *Equilibrium and nonequilibrium statistical mechanics.* Wiley-Interscience, 1975.

[3] A. Bhom and M. Gadella. *Dirac Ket, Gamow Vectors and Gelfand Triplets.* Springer Lecture Notes on Physics, Vol.348. Springer-Verlag, New York, 1989.

[4] C. Chandre and H.R. Jauslin. A universal instability of many-dimensional oscillator systems. *Physics Reports*, 365:1–64, 2002.

[5] B.V. Chirikov. A universal instability of many-dimensional oscillator systems. *Physics Reports*, 52:263, 1979.

[6] D.F. Escande. Stochasticity in classical hamiltonian systems: universal aspects. *Physics Reports*, 121:165, 1985.

[7] L. Van Hove. Quantum-mechanical perturbations giving rise to a statistical transport equations. *Physica*, 21:517, 1955.

[8] L. Van Hove. The approach to equilibrium in quantum statistics. *Physica*, 23:441, 1957.

[9] A.J. Lichtenberg and M.A. Lieberman. *Regular and chaotic dynamics.* Applied Mathematical Sciences. Springer-Verlag, 1992.

[10] G. Ordonez, T. Petrosky, and I. Prigogine. Quantum transitions and dressed unstable states. *Phys. Rev. A*, 63:052106, 2001.

[11] T. Petrosky and H. Hasegawa. Subdynamics and nonintegrable systems. *Physica*, 160A:351, 1989.

[12] T. Petrosky, G. Ordonez, and I. Prigogine. Space time formulation of quantum transitions. *Phys. Rev. A*, 64:062101, 2001.

[13] T. Petrosky and I. Prigogine. Poincaré resonance and the extension of classical dynamics. *Chaos, Solitons and Fractals*, 7:441, 1996.

[14] T. Petrosky and I. Prigogine. The liouville space extension of quantum mechanics. *Advances in Chemical Physics, Vol. 99, eds. I. Prigogine and S. Rice (John Wiley and Sons)*, page 1, 1997.

[15] T. Petrosky, I. Prigogine, and S. Tasaki. Quantum theory of non-integrable systems. *Physica*, 173A:175, 1991.

[16] H. Poincaré. *Méthodes Nouvelles de la Mécanique Céleste.* Gauthier-Villars, 1892; reprinted by Dover, New York, 1957.

[17] I. Prigogine. *Non-equilibrium statistical mechanics.* Monographs in statistical physics and thermodynamics. Interscience, 1962.

[18] I. Prigogine, C. George, F. Henine, and L. Rosenfeld. A universal instability of many-dimensional oscillator systems. *Chem. Scr.*, 4:5, 1973.

[19] I. Prigogine, A. Grecos, and C. George. On the relation of dynamics to statistical mechanics. *Celestial Mechanics*, 16:489, 1977.

[20] I. Prigogine and F. Henin. On the transport equation for dilute gases. *Physica*, 24:214, 1958.

[21] I. Prigogine and F. Henin. On the general theory of the approach to equilibrium. *J. Math. Phys.*, 1:349, 1960.

[22] L.E. Reichl. *The transition to chaos: in conservative classical systems: quantum manifestations.* Springer-Verlag, 1992.

[23] E.C.G. Sudarshan. Quantum dynamics, metastable states, and contractive semigroups. *Phys. Rev. A*, 46:37, 1992.

[24] E.C.G. Sudarshan, C. Chiu, and V. Gorinie. Decaying states as complex energy eigenvectors in generalized quantum mechanics. *Phys. Rev. D*, 18:2914, 1978.

[25] E.T. Whittaker. *A treatise on the analytical dynamics of particles and rigid bodies 4ed.* New York Dover, 1944.

Vita

Chun Biu Li was born in Guang Dong, China on 8th Nov 1972. He received the Bachelor of Science degree in physics from the Chinese University of Hong Kong in 1995. He then entered the physics graduate school of the University of Utah in Salt Lake City. After he finished his Master of Science degree in 1997, he applied to the University of Texas at Austin for enrollment in their physics program. He was accepted and started his Ph.D. studies in August, 1997.

Permanent address: The University of Texas at Austin
The Ilya Prigogine Center for Studies in
Statistical Mechanics and Complex Systems
Austin, Texas 78712

This dissertation was typeset with LaTeX[†] by the author.

[†]LaTeX is a document preparation system developed by Leslie Lamport as a special version of Donald Knuth's TeX Program.